Bootstrapped Representations in Reinforcement Learning

Charline Le Lan [1] Stephen Tu [2] Mark Rowland [2]
Anna Harutyunyan [2] Rishabh Agarwal [2] Marc G. Bellemare [2] Will Dabney [2]

Abstract

In reinforcement learning (RL), state representations are key to dealing with large or continuous state spaces. While one of the promises of deep learning algorithms is to automatically construct features well-tuned for the task they try to solve, such a representation might not emerge from end-to-end training of deep RL agents. To mitigate this issue, auxiliary objectives are often incorporated into the learning process and help shape the learnt state representation. Bootstrapping methods are today's method of choice to make these additional predictions. Yet, it is unclear which features these algorithms capture and how they relate to those from other auxiliary-task-based approaches. In this paper, we address this gap and provide a theoretical characterization of the state representation learnt by temporal difference learning (Sutton, 1988). Surprisingly, we find that this representation differs from the features learned by Monte Carlo and residual gradient algorithms for most transition structures of the environment in the policy evaluation setting. We describe the efficacy of these representations for policy evaluation, and use our theoretical analysis to design new auxiliary learning rules. We complement our theoretical results with an empirical comparison of these learning rules for different cumulant functions on classic domains such as the four-room domain (Sutton et al., 1999) and Mountain Car (Moore, 1990).

1. Introduction

The process of representation learning is crucial to the success of reinforcement learning at scale. In deep reinforcement learning, a neural network is used to parameterise a

[1]University of Oxford [2]Google DeepMind. Correspondence to: Charline Le Lan <charline.lelan@stats.ox.ac.uk>.
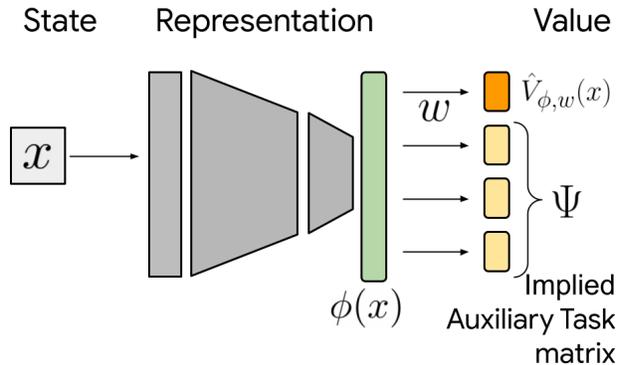
Figure 1: In deep RL, we see the penultimate layer of the network as the representation ϕ which is linearly transformed into a value prediction $\hat{V}_{\phi,w}$ and auxiliary predictions $\Psi(x)$ by bootstrapping methods.

representation ϕ which is linearly mapped into a *value function* (Figure 1) (Yu and Bertsekas, 2009; Bellemare et al., 2019; Levine et al., 2017); this approach often leads to state-of-the-art performance in the field (Mnih et al., 2015). State representations are key to the stability and quality of this learning process.

However, a representation supporting the downstream task of interest might not emerge from end-to-end training. Hence, auxiliary objectives are often incorporated into the training process to help the agent combine its inputs into useful features (Sutton et al., 2011; Jaderberg et al., 2017; Bellemare et al., 2017; Lyle et al., 2021) and the resulting network's representation can help the agent estimate the value function. To construct representations supporting these characteristics, different kind of auxiliary tasks have thus been incorporated into the learning process such as controlling visual aspects of observed states (Jaderberg et al., 2017), predicting the values of several policies (Bellemare et al., 2019; Dabney et al., 2021), predicting values over multiple discount factors (Fedus et al., 2019) or prediction of next state observations (Jaderberg et al., 2017; Gelada et al., 2019) and rewards (Dabney et al., 2021; Lyle et al., 2021; Farebrother et al., 2023).

While these tasks have mainly been trained by bootstrapping, a precise characterization of the representations they learn is lacking. This paper aims to fill this gap. We study

the representations learnt by TD learning when training auxiliary tasks consisting in predicting the expected return of a fixed policy for several cumulant functions (Section 3). More generally, this analysis informs bootstrapped representations arising from algorithms such as Q-learning (Watkins and Dayan, 1992), n-step Q-learning (Hessel et al., 2018; Kapturowski et al., 2019; Schwarzer et al., 2021) or Retrace (Munos et al., 2016). Our key insight is that the way we train these value functions, for instance by TD learning, Monte Carlo or residual gradient, influences the resulting features. In particular, we show that when trained by TD learning, these features converge to the top-d real invariant subspace of the transition matrix P^π, when it exists (Theorem 1). We present an empirical evaluation that supports our theoretical characterizations and show the importance of the choice of a learning rule to learn the value function in Section 5.

In Section 4, we characterise the goodness of these representations by quantifying the approximation error of a linear prediction of the value function from these frozen representations in the TD learning and batch Monte Carlo settings (Subsection 4.1). We find that to minimize this error, the cumulants need to depend on the dynamics of the environment but in a different way whether we learn the main value function by batch Monte Carlo or TD learning. Then, we show random cumulants which have been used in the literature (Lyle et al., 2021; Farebrother et al., 2023) can be good pseudo-reward functions for some particular structures of the successor representation (Dayan, 1993) by providing an error bound that arises from sampling a small number of random pseudo-reward functions (Subsection 4.2).

Finally, we find that one way to improve this bound is to sample pseudo-reward functions which depend on the dynamics of the environment and inspired by this observation, we propose a novel auxiliary task method with adaptive cumulants and show that the resulting pretrained features outperform training from scratch on the Four Rooms and Mountain Car domains Subsection 5.3.

2. Background

We consider a Markov decision process (MDP) $\mathcal{M} = \langle \mathcal{S}, \mathcal{A}, \mathcal{R}, \mathcal{P}, \gamma \rangle$ (Puterman, 1994) with finite state space $\mathcal{S}$, finite set of actions $\mathcal{A}$, transition kernel $\mathcal{P} : \mathcal{S} \times \mathcal{A} \to \mathscr{P}(\mathcal{S})$, deterministic reward function $\mathcal{R} : \mathcal{S} \times \mathcal{A} \to [-R_{\max}, R_{\max}]$, and discount factor $\gamma \in [0, 1)$. A stationary policy $\pi : \mathcal{S} \to \mathscr{P}(\mathcal{A})$ is a mapping from states to distributions over actions, describing a particular way of interacting with the environment. We denote the set of all policies by Π. We write $P_\pi : \mathcal{S} \to \mathscr{P}(\mathcal{S})$ the transition kernel induced by a policy $\pi \in \Pi$

$$P_\pi(s, s') = \sum_{a \in \mathcal{A}} \mathcal{P}(s, a)(s') \pi(a \mid s)$$

and $r_\pi : \mathcal{S} \to [-R_{\max}, R_{\max}]$ the expected reward function

$$r_\pi(s) = \mathbb{E}_\pi[\mathcal{R}(S_0, A_0) \mid S_0 = s, A_0 \sim \pi(\cdot \mid S_0)].$$

For any policy $\pi \in \Pi$, the value function $V^\pi(s)$ measures the expected discounted sum of rewards received when starting from state $s \in \mathcal{S}$ and acting according to π:

$$V^\pi(s) := \mathbb{E}_{\pi, \mathcal{P}} \left[\sum_{t=0}^\infty \gamma^t \mathcal{R}(S_t, A_t) \mid S_0 = s, A_t \sim \pi(\cdot \mid S_t) \right].$$

It satisfies the Bellman equation (Bellman, 1957)

$$V^\pi(s) = r_\pi(s) + \gamma \mathbb{E}_{S' \sim P_\pi(\cdot \mid s)}[V^\pi(S')],$$

which can be expressed using vector notation (Puterman, 1994). Assuming that there are $S = |\mathcal{S}|$ states and viewing r_π and V^π as vectors in $\mathbb{R}^S$ and P_π as an $\mathbb{R}^{S \times S}$ transition matrix, we have

$$V^\pi = r_\pi + \gamma P_\pi V^\pi = (I - \gamma P_\pi)^{-1} r_\pi.$$

We are interested in approximating the value function V^π using a linear combination of features (Yu and Bertsekas, 2009; Levine et al., 2017; Bellemare et al., 2019). We call the mapping $\phi : \mathcal{S} \to \mathbb{R}^d$ a *state representation*, where $d \in \mathbb{N}^+$. Usually, we are interested in reducing the number of parameters needed to approximate the value function and have $d \ll S$. Given a feature vector $\phi(s)$ for a state $s \in \mathcal{S}$ and a weight vector $w \in \mathbb{R}^d$, the value function approximant at s can be expressed as

$$V_{\phi, w}(s) = \phi(s)^\top w.$$

We write the *feature matrix* $\Phi \in \mathbb{R}^{S \times d}$ whose rows correspond to the per-state feature vectors $(\phi(s), s \in \mathcal{S})$. This leads to the more concise value function approximation

$$V_{\phi, w} = \Phi w.$$

In the classic linear function approximation literature, the feature map ϕ is held fixed, and the agent adapts only the weights w to attempt to improve its predictions. By contrast, in deep reinforcement learning, ϕ itself is parameterized by a neural network and is typically updated alongside w to improve predictions about the value function.

We measure the accuracy of the linear approximation $V_{\phi, w}$ in terms of the squared ξ-weighted l_2 norm, for $\xi \in \mathscr{P}(\mathcal{S})$,[1]

$$\|V_{\phi, w} - V^\pi\|_\xi^2 = \sum_{s \in \mathcal{S}} \xi(s)(\phi(s)^\top w - V^\pi(s))^2.$$

The ξ-weighted norm describes the importance of each state.

---

[1] We assume that $\xi(s) > 0$ for all states $s \in \mathcal{S}$.

2.1. Auxiliary Tasks

In deep reinforcement learning, the agent can use its representation ϕ to make additional predictions on a set of T auxiliary task functions $\{\psi_t \in \mathbb{R}^S\}_{t \in \{1,...,T\}}$ where each ψ_t maps states to real values (Jaderberg et al., 2017; Bellemare et al., 2019; Dabney et al., 2021). These predictions are used to refine the representation itself. We collect these targets into an *auxiliary task matrix* $\Psi \in \mathbb{R}^{S \times T}$ whose rows are $\psi(s) = [\psi_1(s), ..., \psi_T(s)]$. We are interested in the case of linear task approximation

$$\hat{\Psi} = \Phi W,$$

where $W \in \mathbb{R}^{d \times T}$ is a weight matrix, and want to choose Φ and W such that $\hat{\Psi} \approx \Psi^\pi$. In this paper, we consider a variety of auxiliary tasks that ultimately involve predicting the value functions of auxiliary *cumulants*, also referred to as general value functions (GVFs; Sutton et al., 2011). By construction, these tasks can be decomposed into a non-zero cumulant function $g : \mathcal{S} \rightarrow \mathbb{R}^T$, mapping each state to T real values, and an expected discounted next-state term when acting according to π

$$\psi^\pi(s) = g(s) + \gamma \mathbb{E}_{S' \sim P_\pi(\cdot|s)}[\psi^\pi(S')].$$

In matrix form, this recurrence can be expressed as follows

$$\Psi^\pi = G + \gamma P_\pi \Psi^\pi = (I - \gamma P^\pi)^{-1} G,$$

where $G \in \mathbb{R}^{S \times T}$ is a *cumulant matrix* whose columns correspond to each pseudo-reward vector. An example of a family of auxiliary tasks following this structure is the successor representation (SR) (Dayan, 1993). The SR encodes a state in terms of the expected discounted time spent in other states and satisfies the following recursive form

$$\psi^\pi(s, s'') = \mathbb{I}[s = s''] + \gamma \mathbb{E}_{S' \sim P_\pi(\cdot|s)}[\psi^\pi(S', s'')],$$

for all $s'' \in \mathcal{S}$. The SR is a collection of value functions associated with the cumulant matrix $G = I$. Here we focus our analysis in its tabular form, noting that it can be extended to larger state spaces in a number of ways (Barreto et al., 2017; Janner et al., 2020; Blier et al., 2021; Thakoor et al., 2022; Farebrother et al., 2023).

2.2. Monte Carlo Representations

To understand how auxiliary tasks shape representations, we start by presenting the simple case where the values of auxiliary cumulants are predicted in a supervised way. Here, the targets $\Psi^\pi = (I - \gamma P^\pi)^{-1} G$ are obtained by Monte Carlo rollouts, that is using the fixed policy to perform roll-outs and collecting the sum of rewards. The goal is to minimize the loss below

$$\mathcal{L}_{\text{aux}}^{\text{MC}}(\Phi, W) = \min_{W \in \mathbb{R}^{d \times T}} \|\Xi^{1/2}(\Phi W - \Psi^\pi)\|_F^2.$$

This method results in the network's representation Φ, assuming a linear, fully-connected last layer, corresponding to the k principal components of the auxiliary task matrix Ψ^π if the network is other unconstrained (Bellemare et al., 2019).

Proposition 1 (Monte Carlo representations)**.** *If* $\text{rank}(\Psi^\pi) \geqslant d \geqslant 1$, *all representations spanning the top-d left singular vectors of Ψ^π with respect to the inner product $\langle x, y \rangle_\Xi$ are global minimizers of $\mathcal{L}_{\text{aux}}^{\text{MC}}$ and can be recovered by stochastic gradient descent.*

In large environments, it is not practical to collect full trajectories to estimate Ψ^π. Instead, practitioners learn them by bootstrapping (Sutton and Barto, 1998).

2.3. Temporal Difference Learning with a Deep Network

Temporal difference (TD; Sutton, 1988) is the method of choice for these auxiliary predictions. The main idea of this approach is *bootstrapping* (Sutton and Barto, 1998). It consists in using the current estimate of the auxiliary task function to generate some targets replacing their true value Ψ^π in order to learn a new approximant of the auxiliary task function. In this paper, we consider one-step temporal difference learning where we replace the targets by a one-step prediction from the currently approximated auxiliary task function. The analysis can easily be extended to n-step temporal difference learning; see Appendix G for further details. In deep reinforcement learning, both the representation ϕ and the weights W are learnt simultaneously by minimizing the following loss function

$$\mathcal{L}_{\text{aux}}^{\text{TD}}(\phi, W) = \mathbb{E}_{\substack{s \sim \xi \\ s' \sim P_\pi(\cdot|s)}} \left[\phi(s)W - \text{SG}(g(s) + \gamma\phi(s')W)\right]^2$$

where SG denotes a *stop gradient* and means that ϕ and W are treated as a constant when taking the gradient from automatic differentiation tools (Bradbury et al., 2018; Abadi et al., 2016; Paszke et al., 2019). Written in matrix form, we have

$$\mathcal{L}_{\text{aux}}^{\text{TD}}(\Phi, W) = \|(\Xi)^{\frac{1}{2}}(\Phi W - \text{SG}(G + \gamma P^\pi \Phi W))\|_F^2$$

Here, $\Xi \in \mathbb{R}^{S \times S}$ is a diagonal matrix with elements $\{\xi(s) : s \in \mathcal{S}\}$ on the diagonal. For clarity of exposition, we express this loss with universal value functions but the analysis can be extented to state-action values at the cost of additional complexity. The idea is to reduce the mean squared error between the approximant $\hat{\psi}$ and the target values by stochastic gradient descent (SGD). Taking the gradient of $\mathcal{L}$ with respect to Φ and W, we obtain the *semi-gradient* update rule

$$\Phi \leftarrow \Phi - \alpha\Xi\left((I - \gamma P^\pi)\Phi W - G\right)W^\top$$
$$W \leftarrow W - \alpha\Phi^\top\Xi\left((I - \gamma P^\pi)\Phi W - G\right) \quad (1)$$

for a step size α. Because the values of the targets change over time, the loss $\mathcal{L}$ does not have a proper gradient field (Dann et al., 2014) except in some particular cases (Barnard, 1993; Ollivier, 2018) and hence classic analysis of stochastic gradient descent (Bottou et al., 2018) does not apply.

3. Bootstrapped Representations

We now study the d-dimensional features that arise when performing value estimation of a fixed set of cumulants and how the choice of a learning method such as TD learning affects the learnt representations. Our first result characterizes representations that bootstrap themselves. We assume that the features Φ are updated in a tabular manner under the dynamics in Equation (1). To simplify the presentation, we now make the following invertibility assumption.

Assumption 1. *We assume that $\Phi^{\mathsf{T}}\Xi(I - \gamma P^{\pi})\Phi$ is invertible for any full rank representation $\Phi \in \mathbb{R}^{S \times d}$.*

This standard assumption is for instance verified when ξ is the stationary distribution over states under π of an aperiodic, irreducible Markov chain (see e.g. Sutton et al., 2016).

An interesting characterization of the dynamical system in Equation (1) is its set of critical points. For a given Φ, we write

$$W_{\Phi,G}^{\mathrm{TD}} \in \{W \in \mathbb{R}^{d \times T} | \nabla_W \mathcal{L}_{\mathrm{aux}}^{\mathrm{TD}}(\Phi, W) = 0\}.$$

Using classic linear algebra, we find that the weights W_{TD} obtained at convergence correspond to the LSTD solution (Bradtke and Barto, 1996; Boyan, 2002; Zhang et al., 2021)

$$W_{\Phi,G}^{\mathrm{TD}} = \left(\Phi^{\mathsf{T}}\Xi(I - \gamma P^{\pi})\Phi\right)^{-1} \Phi^{\mathsf{T}}\Xi G.$$

A key notion for our analysis is the concept of *invariant subspace* of a linear mapping.

Definition 1 (Gohberg et al., 2006). *A representation $\Phi \in \mathbb{R}^{S \times d}$ spans a real invariant subspace of a linear mapping $M : \mathcal{S} \to \mathbb{R}^S$ if the column span of Φ is preserved by M, that is in matrix form*

$$\mathrm{span}(M\Phi) \subseteq \mathrm{span}(\Phi).$$

For instance, any real eigenvector of M generates one of its one-dimensional real invariant subspaces.

We are now equipped with the tools to enumerate the set of *critical representations* $\{\Phi \in \mathbb{R}^{S \times d} \mid \nabla_{\Phi}\mathcal{L}_{\mathrm{aux}}^{\mathrm{TD}}(\Phi, W_{\Phi}^{\mathrm{TD}}) = 0\}$ in the lemma below.

Lemma 1 (Critical representations for TD). *All full rank representations which are critical points to $\mathcal{L}_{\mathrm{aux}}^{\mathrm{TD}}$ span real invariant subspaces of $(I - \gamma P^{\pi})^{-1}GG^{\mathsf{T}}\Xi$, that is $\mathrm{span}((I - \gamma P^{\pi})^{-1}GG^{\mathsf{T}}\Xi\Phi) \subseteq \mathrm{span}(\Phi)$.*

Proof. The proof is given in Appendix C and relies on the view of LSTD as an oblique projection (Scherrer, 2010). $\square$

In the particular case of an identity cumulant matrix and a uniform distribution over states, this set can be more directly expressed as the representations invariant under the transition dynamics.

Corollary 1. *If $G = I$ and $\Xi = I/S$, all full rank representations which are critical points to $\mathcal{L}_{\mathrm{aux}}^{\mathrm{TD}}$ span real invariant subspaces of the invariant subspaces of P^{π}.*

Similarly to how the top principal components of a matrix explain most of its variability (Hotelling, 1933), these critical representations are not equally informative of the dynamics of the environment. This motivates the need to understand the behavior of the updates from Equation (1). To ease the analysis, we assume that the weights W have converged perfectly to $W_{\Phi,G}^{\mathrm{TD}}$ at each time step (Le Lan et al., 2023) and consider the following continuous-time dynamics.

$$\frac{d}{dt}\Phi = -\nabla_{\Phi}\mathcal{L}(\Phi, W_{\Phi,G}^{\mathrm{TD}}) = -F(\Phi), \qquad (2)$$

where:

$$F(\Phi) := 2\Xi\left((I - \gamma P^{\pi})\Phi W_{\Phi,G}^{\mathrm{TD}} - G\right)(W_{\Phi,G}^{\mathrm{TD}})^{\mathsf{T}}.$$

We can characterize the behavior of the above critical representations in terms of the notion of *top-d invariant subspace* of P^{π}.

Definition 2 (Top-d invariant subspace). *Let $\lambda_1, \ldots, \lambda_S$ be the (possibly complex) eigenvalues of a linear mapping $M : \mathcal{S} \to \mathbb{R}^S$, ordered by decreasing real part $\mathrm{Re}(\lambda_i) \geq \mathrm{Re}(\lambda_{i+1})$, $i \in \{1, \ldots, S\}$. Assume that $\mathrm{Re}(\lambda_d) > \mathrm{Re}(\lambda_{d+1})$. A representation $\Phi \in \mathbb{R}^{S \times d}$ spans a top-d invariant subspace of M if (i) it is an M-invariant subspace and (ii) $\mathrm{span}(\Phi) \cap \mathrm{span}(v_j) = \{0\}$ for all $j \in \{d + 1, \ldots, S\}$, where v_j is a corresponding eigenvector for eigenvalue λ_j.*

Our key result is that certain non top-d invariant subspaces of P^{π} correspond to unstable critical points of the ordinary differential equation 2.

Theorem 1 (TD representations). *Assume P^{π} real diagonalisable, $G = I$ and a uniform distribution ξ over states. Let $(v_1, \ldots, v_S)$ denote the eigenvectors of P^{π} corresponding to the eigenvalues $(\lambda_1, \ldots, \lambda_S)$. Under the dynamics in Equation (2), all real invariant subspaces of dimension d are critical points, and any real non top-d invariant subspace $\Phi = (v_{i_1}, \ldots, v_{i_d})$ is unstable for gradient descent.*

The result above takes a step toward establishing that the TD algorithm converges towards a real top-d invariant subspace
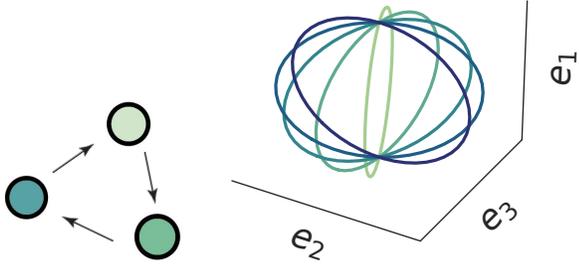
Figure 2: **Left**: A simple 3-state MDP. **Right**: Five subspaces, each represented by a circle, spanned by Φ during the last training steps of gradient descent on $\mathcal{L}_{\mathrm{aux}}^{\mathrm{TD}}$ for $d = 2$.

or diverges with probability 1. While real diagonalisable transition matrices always induce real invariant subspaces, complex eigenvalues do not guarantee their existence and in such a case, where there is no top-d real invariant subspace, the representation learning algorithm *does not converge*. As an illustration, consider the three-state MDP depicted in Figure 2, left, whose transition matrix is complex diagonalisable and given by

$$P^\pi = \begin{bmatrix} 0 & 1 & 0 \\ 0 & 0 & 1 \\ 1 & 0 & 0 \end{bmatrix}$$

Its eigenvalues are $\lambda_1 = 1$ associated to the real eigenvector e_1 and the complex conjugate pair $(\lambda_2, \overline{\lambda_2}) = (e^{2\pi i/3}, e^{-2\pi i/3})$, associated to the pair of real eigenvectors (e_2, e_3). Hence, the real invariant subspaces of P^π are $\{0\}, \mathrm{span}(e_1), \mathrm{span}(e_2, e_3), \mathrm{span}(e_1, e_2, e_3)$. Note that there is no 2-dimensional real invariant subspace containing the top eigenvector e_1. Consequently, the 2-dimensional representation learnt by gradient descent on the TD learning rule with $G = I$ does not converge and rotates in the higher dimensional subspace $\mathrm{span}(e_1, e_2, e_3)$ (see Figure 2, right).

To understand the importance of the stop-gradient in TD learning, it useful to study the representations arising from the minimization of the following loss function

$$\mathcal{L}_{\mathrm{aux}}^{\mathrm{res}}(\Phi, W) = \|\Xi^{\frac{1}{2}} \left(\Phi W - (G + \gamma P^\pi \Phi W)\right)\|_F^2,$$

which corresponds to residual gradient algorithms (Baird, 1995). While it has been remarked on before that the weights minimizing $\mathcal{L}_{\mathrm{aux}}^{\mathrm{res}}(\Phi, W)$ for a fixed Φ differ from $W_{\Phi,G}^{\mathrm{TD}}$ (see Lemma 8; Lagoudakis and Parr, 2003; Scherrer, 2010), this objective function also has a different optimal representation

Proposition 2 (Residual representations). *Let* $d \in \{1, ..., S\}$ *and* F_d *be the top* d *left singular vectors of* G *with respect to the inner product* $\langle x, y \rangle_\Xi = y^\mathsf{T}\Xi x$, *for all* $x, y \in \mathbb{R}^S$. *All representations spanning* $(I - \gamma P^\pi)^{-1}F_d$

are global minimizers of $\mathcal{L}_{\mathrm{aux}}^{\mathrm{res}}$ and can be recovered by stochastic gradient descent.

While TD and Monte Carlo representations are in general different, in the particular case of symmetric transition matrices and orthogonal cumulant matrices, they are the same.

Corollary 2 (Symmetric transition matrices). *If a cumulant matrix* $G \in \mathbb{R}^{S \times T}$ *(with* $T \geqslant S$*) has unit-norm, orthogonal columns (e.g.* $G = I$*), the representations learnt from the supervised objective* $\mathcal{L}_{\mathrm{aux}}^{\mathrm{MC}}$ *and the TD update rule* $\mathcal{L}_{\mathrm{aux}}^{\mathrm{TD}}$ *are the same for symmetric transition matrices* P^π *under a uniform state distribution* ξ.

This is because eigenvectors and singular vectors are identical in that setting and the eigenvalues of the successor representation are all positive.

4. Representations for Policy Evaluation

With the results from the previous section, the question that naturally arises is which approach results in better representations. To provide an answer, we consider a two-stage procedure. First, we learn a representation Φ by predicting the values of T auxiliary cumulants simultaneously, using one of the learning rules described in Section 3. Then, we retain this representation and perform policy evaluation. If the value function is estimated on-policy, it converges towards the LSTD solution (Tsitsiklis and Van Roy, 1996)

$$\hat{V}^{\mathrm{TD}} = \Phi w_\Phi^{\mathrm{TD}}$$

where $w_\Phi^{\mathrm{TD}} = \left(\Phi^\mathsf{T}\Xi(I - \gamma P^\pi)\Phi\right)^{-1}\Phi^\mathsf{T}\Xi r_\pi$. We are interested in whether this value function results in low approximation error on average over random reward functions.

Definition 3 (l_1-ball optimal representation for TD). *We say that a representation* Φ_{TD}^* *is* l_1*-ball optimal for TD learning when it minimizes the error*

$$\mathbb{E}_{r_\pi}[\|\Phi w_\Phi^{\mathrm{TD}} - V^\pi\|_\xi^2] \tag{3}$$

where the expectation is over the reward functions r_π *sampled uniformly over the* l_1*-ball* $\{r_\pi \in \mathbb{R}^S \mid \|r_\pi\|_1 \leqslant 1\}$.

This set of rewards models an unknown reward function. Here Φ_{TD}^* depends on the transition dynamics of the environment but not on the reward function.

Lemma 2. *A representation* Φ_{TD}^* *is* l_1*-ball optimal for TD learning iff it is a solution of the following optimization problem.*

$$\Phi_{\mathrm{TD}}^* \in \arg\min\nolimits_\Phi \left\|\Xi^{1/2}(\Phi W_{\Phi,I}^{\mathrm{TD}} - (I - \gamma P^\pi)^{-1})\right\|_F^2.$$

When P^π is symmetric and $\Xi = I/|\mathcal{S}|$, the minimum is achieved by both the top-d left singular vectors and top-d

MAIN ALGORITHM	l_1-BALL OPTIMAL REPRESENTATION	REPRESENTATION LOSS	LEARNT REPRESENTATION
BATCH MC	$\mathrm{SVD}\left((I - \gamma P^\pi)^{-1}\right)$	MC	$\mathrm{SVD}\left((I - \gamma P^\pi)^{-1} G\right)$
RESIDUAL	$\mathrm{SVD}\left((I - \gamma P^\pi)^{-1}\right)\Sigma_d$	RESIDUAL	$(I - \gamma P^\pi)^{-1}\,\mathrm{SVD}\,(G)$
TD	Φ^*_{TD}	TD	$\mathrm{INV}\left((I - \gamma P^\pi)^{-1} GG^\mathsf{T}\Xi\right)$

Table 1: Different types of representation loss and their induced representations. The supervised targets $\Psi \in \mathbb{R}^{S \times T}$ are $(I - \gamma P^\pi)^{-1} G$. $\mathrm{SVD}(M)$ denotes the top-d left singular vectors of M, $\mathrm{INV}(M)$ the top-d invariant subspace of M and $\Sigma_d \in \mathbb{R}^{d \times d}$ the diagonal matrix with the top-d singular values of $(I - \gamma P^\pi)^{-1}$ on its diagonal.

invariant subspace of the SR. However, as the misalignment between the top-d left and top-d right singular vectors of $(I - \gamma P^\pi)$ increases, the top-d invariant subspace results in lower error compared to the top-d singular vectors (see Figure 3); note that here, none of them achieves Φ^*_{TD} and hence $G = I$ is not l_1-ball optimal for TD learning. As
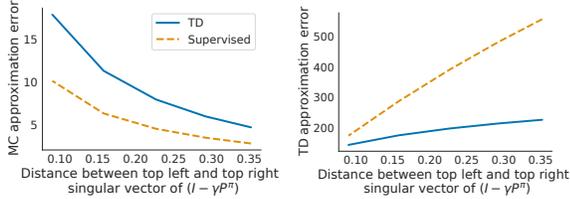

Figure 3: MC (**left**) and TD (**right**) approximation errors as a function of the misalignment of the top left and right singular vector of the SR induced by greedifying the policy. Trained with $\mathcal{L}^{\mathrm{MC}}_{\mathrm{aux}}$, $\mathcal{L}^{\mathrm{TD}}_{\mathrm{aux}}$, $G = I$, $d = 1$ on a 4-state room.

a comparison, we study which representations are l_1-ball optimal for linear batch Monte Carlo policy evaluation. In that setting, we are given a dataset consisting of states and their associated value, which can be estimated by the realisation of the random return (Bellemare et al., 2017; Sutton and Barto, 2018), and the weights are learnt by least square regression. As above, we want the features minimizing the resuting approximation error averaged over a set of possible reward functions.

Definition 4 (l_1-ball optimal representation for MC). *We say that a representation $\Phi^*_{\Phi_{\mathrm{MC}}}$ is l_1-ball optimal for batch Monte Carlo when it minimizes the error*

$$\mathbb{E}_{\|r_\pi\|_1 \leqslant 1}[\|\Phi w^{\mathrm{MC}}_\Phi - V^\pi\|^2_\xi] \tag{4}$$

where $\hat{V}^{\mathrm{MC}} = \Phi w^{\mathrm{MC}}_\Phi$ is the value function learnt at convergence and $w^{\mathrm{MC}}_\Phi = (\Phi^\top \Xi \Phi)^{-1}\Phi^\top \Xi V^\pi$.

Unlike TD, a representation Φ^*_{MC} is can be learnt by training $\mathcal{L}^{\mathrm{MC}}_{\mathrm{aux}}$ with $G = I$.

Lemma 3. *A representation Φ^*_{MC} is l_1-ball optimal for batch Monte Carlo policy evaluation if its column space spans the top-d left singular vectors (with respect to the inner product $\langle x, y \rangle_\Xi$) of $(I - \gamma P^\pi)^{-1}$.*

We summarize in Table 1 our representation learning results mentioned throughout Section 3 and Section 4. For completeness, we also include l_1-ball optimal representations for residual algorithms. Proofs can be found in Appendix D.

4.1. TD and Monte Carlo Need Different Cumulants

Having characterized which features common auxiliary tasks capture and what representations are desirable to support training the main value function, we now show that MC policy evaluation and TD learning need different cumulants. In large environments, we are interested in cumulant matrices encoding a small number of tasks $T \ll S$.

Lemma 4. *Denote B_T the top-T right singular vectors of the SR and $\mathcal{O}(T, S)$ the set of orthogonal matrices in $\mathbb{R}^{T \times S}$. Training auxiliary tasks in a MC way with any G from the set $\{G \in \mathbb{R}^{S \times T} | \exists M \in \mathcal{O}(T, S), G = B_T M\}$ results in an l_1-ball optimal representation for batch Monte Carlo.*

We showed in Section 3 that training auxiliary tasks by TD does not always converge when the transition matrix has complex eigenvalues. Maybe surprisingly, we find that this is not problematic when learning the main value function by TD. Indeed, the rotation of its own weights balances the rotation of the underlying representation.

Lemma 5. *Let $\{\Phi_\omega\}$ be the set of rotating representations from Figure 2 learnt by TD learning with $G = I$ and $d = 2$. All these representations are equally good for learning the main value function by TD learning, that is $\forall \omega \in [0, 1]$,*

$$\mathbb{E}_{\|r\|^2_2 < 1}\left\|\Phi_\omega w^{\mathrm{TD}}_{\Phi_\omega} - V^\pi\right\|^2_F$$

is constant and independent of ω.

Although $G = I$ does not always lead to Φ^*_{TD} when training $\mathcal{L}^{\mathrm{TD}}_{\mathrm{aux}}$, by analogy with the MC setting, we assume that $G = I$ leads to overall desirable representations. Assuming $\Xi = I/|\mathcal{S}|$, this means we would like the subspace spanned by top-d invariant subspaces of $(I - \gamma P^\pi)^{-1}$ to be the same as the subspace spanned by the top d invariant subspaces of $(I - \gamma P^\pi)^{-1} GG^\top$.

Lemma 6. *The set of cumulant matrices $G \in \mathbb{R}^{S \times T}$ that preserve the top-T invariant subspaces of the successor representation by TD learning are the top-T orthogonal invariant subspaces of $(I - \gamma P^\pi)^{-1}$, that is satisfying $G^\top G = I$*

6
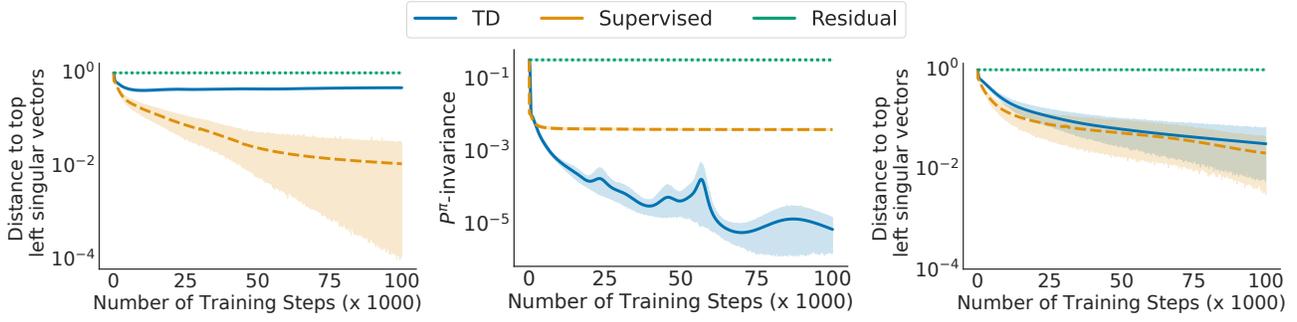
Figure 4: Subspace distance between Φ and the top-d left singular vectors of the SR on the **left** (resp. and a top-d P^π-invariant subspace in the **middle** over the course of training $\mathcal{L}_{\text{aux}}^{\text{TD}}$, $\mathcal{L}_{\text{aux}}^{\text{MC}}$ and $\mathcal{L}_{\text{aux}}^{\text{res}}$ for 10^5 steps, averaged over 30 seeds ($d = 3$). MDPs with real diagonalisable (**left, middle**) and symmetric (**right**) transition matrices are randomly generated. Shaded areas represent 95% confidence intervals.

by orthogonality and $(I - \gamma P^\pi)^{-1} G \subseteq G$ by the invariance property.

Unlike the MC case, a desirable cumulant matrix should encode the exact same information as the representation being learnt and the choice of a parametrization here matters.

4.2. A Deeper Analysis of Random Cumulants

We now study random cumulants which have mainly been used in the literature (Dabney et al., 2021; Lyle et al., 2021; Farebrother et al., 2023) as a heuristic to learn representations. We aim to explain their recent achievements as a pretraining technique (Farebrother et al., 2023) and their effectiveness in sparse reward environments (Lyle et al., 2021).

Proposition 3 (MC Error bound). *Let $G \in \mathbb{R}^{S \times T}$ be a sample from a standard gaussian distribution and assume $d \leqslant T$. Let F_d be the top-d left singular vectors of the successor representation $(I - \gamma P^\pi)^{-1}$ and $\hat{F}_d$ be the top left singular vectors of $(I - \gamma P^\pi)^{-1} G$. Denote $\sigma_1 \geqslant \sigma_2 \geqslant \ldots \geqslant \sigma_S$ the singular values of the SR and $\mathrm{dist}(F_d, \hat{F}_d)$ the $\sin \theta$ distance between the subspaces spanned by F_d and $\hat{F}_d$. Denoting $p = T - d$, we have*

$$\mathbb{E}[\mathrm{dist}(F_d, \hat{F}_d)] \leqslant \sqrt{\frac{d}{p-1}} \frac{\sigma_{d+1}}{\sigma_d} + \frac{e\sqrt{T}}{p} \left(\sum_{j=d+1}^{n} \frac{\sigma_j^2}{\sigma_d^2} \right)^{\frac{1}{2}}$$

Proof. A proof can be found in Appendix E and follows arguments from random matrix theory. □

This bound fundamentally depends on the ratio of the singular values σ_{d+1}/σ_d of the successor representation. As the oversampling parameter $(T - d)$ grows, the right hand side tends towards 0. In particular, for the right hand side to be less than ϵ, we need the oversampling parameter to satisfy $(T - d) \geqslant 1/\epsilon^2$. We investigate to which extent this result holds empirically for the TD objective in Subsection 4.1.

5. Empirical Analysis

In this section, we illustrate empirically the correctness of our theoretical characterizations from Section 3 and compare the goodness of different cumulants on the four room (Sutton and Barto, 2018) and Mountain car (Moore, 1990) domains. Let $P_\Phi = \Phi(\Phi^\top \Phi)^\dagger \Phi^\top$. Here, any distance between two subspaces Φ and Φ^* is measured using the normalized subspace distance, [2] (Tang, 2019) defined by

$$\mathrm{dist}(\Phi, \Phi^*) = 1 - \frac{1}{d} \cdot \mathrm{Tr}\left(P_{\Phi^*} P_\Phi \right) \in [0, 1].$$

5.1. Synthetic Matrices

To begin, we train the TD, supervised and residual update rules from Section 3 up to convergence knowing the exact transition matrices P^π. In Figure 4 left and middle, we randomly sample 30 real diagonalisable matrices $P^\pi \in \mathbb{R}^{50 \times 50}$ to prevent any convergence issue from the TD update rule. In Figure 4 right, we generate symmetric transition matrices $P^\pi \in \mathbb{R}^{50 \times 50}$. To illustrate the theory, we run gradient descent on each learning rule by expressing the weights implicitly as a function of the features (see Equation (2) for TD for instance). Figure 4, left, middle show that these auxiliary task algorithms learn different representations and successfully recover our theoretical characterizations (Proposition 1, Theorem 1) from Table 1, right. Figure 4 right illustrates that the supervised and TD rules converge to the same representation for symmetric P^π, as predicted by our theory (Corollary 2).

5.2. Efficacy of Random Cumulants

Following our theoretical analysis from Subsection 5.2, our aim is to illustrate the goodness of random cumulants at recovering the left singular vectors of the successor representation on the four room domain (Sutton et al., 1999)

[2] It is equivalent to the $\sin \theta$ distance up to some constant
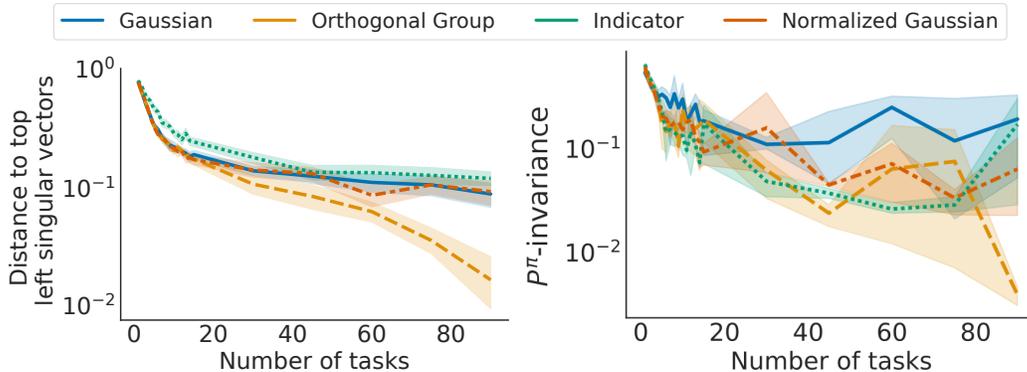
Figure 5: Subspace distance after 5×10^5 training steps and averaged over 30 seeds ($d = 5$) between Φ learnt with $\mathcal{L}_{\text{aux}}^{\text{MC}}$ and the top left singular vectors of the SR (**left**) and between Φ learnt with $\mathcal{L}_{\text{aux}}^{\text{TD}}$ and the top invariant subspaces of the SR (**right**) for different random cumulants, on the four-room domain. Shaded areas represent estimates of 95% confidence intervals

and to investigate to which extent an analogous result holds empirically for the TD rule. We investigate the importance of three properties of a distribution: isotropy, norm and orthogonality of the columns. We consider random cumulants from different distributions: a standard Gaussian $\mathbb{N}(0, I)$, a Gaussian distribution which columns are normalized to be unit-norm, the $O(N)$ Haar distribution and random indicators functions. Figure 5, left shows that the the indicator distribution which is not isotropic performs worse overall for the supervised objective and when the number of tasks is large enough, orthogonality between the columns of the cumulant matrix leads to better accuracy. In comparison, Figure 5, right studies the goodness of random cumulants at recovering the top-d invariant subspaces of the SR and depicts a different picture. Here, the Gaussian distribution achieves the highest error irrespective of the number of tasks sampled while the normalized Gaussian achieves lower error suggesting the norm of the columns matter for TD training. The indicator distribution performs well for many number of sampled tasks indicating that the isotropy of the distribution is not as important for TD as it is for supervised training. Finally, the orthogonal cumulants achieve the lowest error when the number of tasks is large enough, showing this is an important property for both kinds of training.

5.3. Offline Pre-training

In this section we follow a similar evaluation protocol as that of Farebrother et al. (2023), but applied to the four room and Mountain car domains to allow a clear investigation of the various cumulant generation methods and the effects of their corresponding GVFs as a representation pre-training method for reinforcement learning. Details can be found in Appendix A.

We consider four cumulant functions. The first two are stationary and are generated before offline pre-training begins. For ExactSVD, we compute the top-k right singular vectors

of the successor representation matrix of the uniform random policy. For Normal, we generate cumulant functions sampled from a standard Normal distribution.

The second two cumulant functions are learned during offline pre-training using a separate neural network. RNI (Farebrother et al., 2023), learns a set of indicator functions which are trained to be active in a particular percentage of the states (15% in this experiment). Clustering Contrastive Representations (CCR) learns cumulants by learning a representation of the state using CPC (Oord et al., 2018), and then performs online clustering of the learned representations with k clusters. The online clustering method we use differs slightly from standard approaches in that we maintain an estimate of the frequency that each cluster center is assigned to a state, p_i, and the assigned cluster is identified with $\arg\min_i p_i \| \phi(x) - b_i \|$, where $\phi(x)$ is the learned CPC representation and b_i is cumulant i's centroid. Examples of the cumulants produced by these four methods, and their corresponding value functions, are given in Appendix A.

Figure 6 compares the online performance after pre-training, for various cumulant functions, with the online performance of DQN without pre-training. Two take-aways are readily apparent. First, that offline pre-training, speeds up online learning, as expected. Second, that the two best performing methods are both sensitive to the structure of the environment dynamics, directly in the case of ExactSVD and indirectly through the CPC representation for CCR.

6. Related Work

Optimal representations. Bellemare et al. (2019) define a notion of optimal representations for batch Monte Carlo optimization based on the worst approximation error of the value function across the set of all possible policies, later relaxed by Dabney et al. (2021). Instead, we do not consider the control setting but focus on policy evaluation. Ghosh
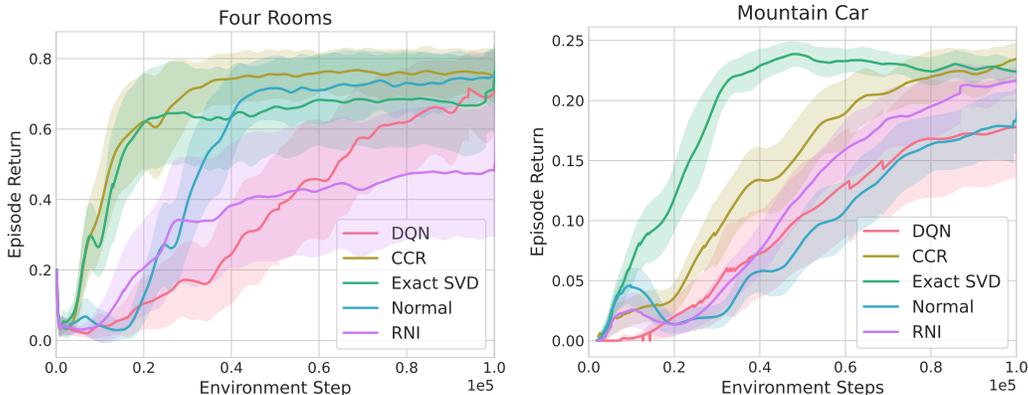
Figure 6: Comparing effects of offline pre-training on the FourRooms (**left**) and sparse Mountain Car (**right**) domains for different cumulant generation methods. Results are averages over 30 seeds.

and Bellemare (2020) and Le Lan et al. (2022) characterize the stability, approximation and generalization errors of the SR (Dayan, 1993) and Schur representations which are P^π-invariant, a key property to ensure stability. In contrast, we formalize that predicting values functions by TD learning from $G = I$ leads to P^π-invariant subspaces.

Auxiliary tasks. Lyle et al. (2021) analyse the representations learnt by several auxiliary tasks such as random cumulants (Osband et al., 2018; Dabney et al., 2021) assuming real diagonalizability of the transition matrix P^π and constant weights W. They found that in the limit of an infinity of gaussian random cumulants, the subspace spanned by TD representations converges in distribution towards the left singular vectors of the successor representation. Instead, our theoretical analysis holds for any transition matrix and both the weights W and the features Φ are updated at each time step. Recently, Farebrother et al. (2023) rely on a random binary cumulant matrix which sparsity is controlled by means of a quantile regression loss. Finally, other auxiliary tasks regroup self-supervised learning methods (Schwarzer et al., 2021; Guo et al., 2020). Tang et al. (2023) demonstrate that these algorithms perform an eigendecompositon of real diagonalisable transition matrix P^π, under some assumptions, suggesting a close connection to TD auxiliary tasks. Closely related, Touati and Ollivier (2021); Blier et al. (2021) propose an unsupervised pretraining algorithm to learn representations based on an eigendecomposition of transition matrix P^π. They demonstrate the usefulness of their approach on discrete and continuous mazes, pixel-based MsPacman and the FetchReach virtual robot arm.

7. Conclusion

In this paper, we have studied representations learnt by bootstrapping methods and proved their benefit for value-based deep RL agents. Based on an analysis of the TD continuous-time dynamical system, we generalized existing work (Lyle et al., 2021) and provided evidence that TD representations are actually different from Monte Carlo representations.

Our investigation demonstrated that an identity cumulant matrix provides as much information as the TD and supervised auxiliary algorithms can carry; this work also shows that it is possible to design more compact pseudo-reward functions, though this requires prior knowledge about the transition dynamics. This led us to propose new families of cumulants which also proved useful empirically.

We assumed in this paper that the TD updates are carried out in tabular way, that is that there is not generalization between states when we update the features. An exciting opportunity for future work is to extend the theoretical results to the case where the representation is parametrized by a neural network. Other avenues for future work include scaling up the representation learning methods here introduced.

References

Abadi, M., Barham, P., Chen, J., Chen, Z., Davis, A., Dean, J., Devin, M., Ghemawat, S., Irving, G., Isard, M., Kudlur, M., Levenberg, J., Monga, R., Moore, S., Murray, D. G., Steiner, B., Tucker, P., Vasudevan, V., Warden, P., Wicke, M., Yu, Y., and Xiaoqiang, Z. (2016). Tensorflow: A system for large-scale machine learning. In *USENIX Symposium on Operating Systems Design and Implementation*.

Baird, L. (1995). Residual algorithms: Reinforcement learning with function approximation. In *Machine Learning Proceedings 1995*, pages 30–37. Elsevier.

Barnard, E. (1993). Temporal-difference methods and markov models. *IEEE Transactions on Systems, Man, and Cybernetics*, 23(2):357–365.

Barreto, A., Dabney, W., Munos, R., Hunt, J. J., Schaul, T., van Hasselt, H. P., and Silver, D. (2017). Successor features for transfer in reinforcement learning. In *Advances in Neural Information Processing Systems*.

Bellemare, M., Dabney, W., Dadashi, R., Ali Taiga, A., Castro, P. S., Le Roux, N., Schuurmans, D., Lattimore, T., and Lyle, C. (2019). A geometric perspective on optimal representations for reinforcement learning. In *Advances in Neural Information Processing Systems*.

Bellemare, M. G., Dabney, W., and Munos, R. (2017). A distributional perspective on reinforcement learning. In *Proceedings of the International Conference on Machine Learning*.

Bellman, R. (1957). Dynamic programming princeton university press princeton. *New Jersey Google Scholar*.

Blier, L., Tallec, C., and Ollivier, Y. (2021). Learning successor states and goal-dependent values: A mathematical viewpoint. *arXiv preprint arXiv:2101.07123*.

Bottou, L., Curtis, F. E., and Nocedal, J. (2018). Optimization methods for large-scale machine learning. *Siam Review*, 60(2):223–311.

Boyan, J. A. (2002). Technical update: Least-squares temporal difference learning. *Machine learning*, 49(2):233–246.

Bradbury, J., Frostig, R., Hawkins, P., Johnson, M. J., Leary, C., Maclaurin, D., Necula, G., Paszke, A., VanderPlas, J., Wanderman-Milne, S., and Zhang, Q. (2018). JAX: composable transformations of Python+NumPy programs.

Bradtke, S. J. and Barto, A. G. (1996). Linear least-squares algorithms for temporal difference learning. *Machine learning*, 22(1):33–57.

Dabney, W., Barreto, A., Rowland, M., Dadashi, R., Quan, J., Bellemare, M. G., and Silver, D. (2021). The value-improvement path: Towards better representations for reinforcement learning. In *Proceedings of the AAAI Conference on Artificial Intelligence*.

Dann, C., Neumann, G., Peters, J., et al. (2014). Policy evaluation with temporal differences: A survey and comparison. *Journal of Machine Learning Research*, 15:809–883.

Dayan, P. (1993). Improving generalization for temporal difference learning: The successor representation. *Neural Computation*, 5(4):613–624.

Farebrother, J., Greaves, J., Agarwal, R., Lan, C. L., Goroshin, R., Castro, P. S., and Bellemare, M. G. (2023). Proto-value networks: Scaling representation learning with auxiliary tasks. In *Proceedings of the International Conference on Learning Representations*.

Fedus, W., Gelada, C., Bengio, Y., Bellemare, M. G., and Larochelle, H. (2019). Hyperbolic discounting and learning over multiple horizons. *arXiv preprint arXiv:1902.06865*.

Ge, R., Jin, C., and Zheng, Y. (2017). No spurious local minima in nonconvex low rank problems: A unified geometric analysis. In *Proceedings of the International Conference on Machine Learning*.

Gelada, C., Kumar, S., Buckman, J., Nachum, O., and Bellemare, M. G. (2019). DeepMDP: Learning continuous latent space models for representation learning. In *Proceedings of the International Conference on Machine Learning*.

Ghosh, D. and Bellemare, M. G. (2020). Representations for stable off-policy reinforcement learning. In *Proceedings of the International Conference on Machine Learning*.

Gohberg, I., Lancaster, P., and Rodman, L. (2006). *Invariant subspaces of matrices with applications*. SIAM.

Guo, Z. D., Pires, B. A., Piot, B., Grill, J.-B., Altché, F., Munos, R., and Azar, M. G. (2020). Bootstrap latent-predictive representations for multitask reinforcement learning. In *Proceedings of the International Conference on Machine Learning*.

Halko, N., Martinsson, P.-G., and Tropp, J. A. (2011). Finding structure with randomness: Probabilistic algorithms for constructing approximate matrix decompositions. *SIAM review*, 53(2):217–288.

Harris, C. R., Millman, K. J., van der Walt, S. J., Gommers, R., Virtanen, P., Cournapeau, D., Wieser, E., Taylor, J., Berg, S., Smith, N. J., et al. (2020). Array programming with numpy. *Nature*, 585(7825):357–362.

Hessel, M., Modayil, J., van Hasselt, H., Schaul, T., Ostrovski, G., Dabney, W., Horgan, D., Piot, B., Azar, M., and Silver, D. (2018). Rainbow: Combining improvements in deep reinforcement learning. In *Proceedings of the AAAI Conference on Artificial Intelligence*.

Hotelling, H. (1933). Analysis of a complex of statistical variables into principal components. *Journal of educational psychology*, 24(6):417.

Hunter, J. D. (2007). Matplotlib: A 2d graphics environment. *Computing in science & engineering*, 9(3):90–95.

Jaderberg, M., Mnih, V., Czarnecki, W. M., Schaul, T., Leibo, J. Z., Silver, D., and Kavukcuoglu, K. (2017). Reinforcement learning with unsupervised auxiliary tasks. In *Proceedings of the International Conference on Learning Representations*.

Janner, M., Mordatch, I., and Levine, S. (2020). Gamma-models: Generative temporal difference learning for infinite-horizon prediction. In *Advances in Neural Information Processing Systems*.

Jin, C., Ge, R., Netrapalli, P., Kakade, S. M., and Jordan, M. I. (2017). How to escape saddle points efficiently. In *Proceedings of the International Conference on Machine Learning*.

Jones, E., Oliphant, T., and Peterson, P. (2001). SciPy: open source scientific tools for Python.

Kapturowski, S., Ostrovski, G., Quan, J., Munos, R., and Dabney, W. (2019). Recurrent experience replay in distributed reinforcement learning. In *Proceedings of the International conference on learning representations*.

Lagoudakis, M. G. and Parr, R. (2003). Least-squares policy iteration. *The Journal of Machine Learning Research*, 4:1107–1149.

Le Lan, C., Greaves, J., Farebrother, J., Rowland, M., Pedregosa, F., Agarwal, R., and Bellemare, M. G. (2023). A novel stochastic gradient descent algorithm for learning principal subspaces. In *Proceedings of the International Conference on Artificial Intelligence and Statistics*.

Le Lan, C., Tu, S., Oberman, A., Agarwal, R., and Bellemare, M. G. (2022). On the generalization of representations in reinforcement learning. In *Proceedings of the International Conference on Artificial Intelligence and Statistics*.

Levine, N., Zahavy, T., Mankowitz, D., Tamar, A., and Mannor, S. (2017). Shallow updates for deep reinforcement learning. In *Advances in Neural Information Processing Systems*.

Lyle, C., Rowland, M., Ostrovski, G., and Dabney, W. (2021). On the effect of auxiliary tasks on representation dynamics. In *Proceedings of the International Conference on Artificial Intelligence and Statistics*.

Mnih, V., Kavukcuoglu, K., Silver, D., Rusu, A. A., Veness, J., Bellemare, M. G., Graves, A., Riedmiller, M., Fidjeland, A. K., Ostrovski, G., Petersen, S., Beattie, C., Sadik, A., Antonoglou, I., King, H., Kumaran, D., Wierstra, D., Legg, S., and Hassabis, D. (2015). Human-level control through deep reinforcement learning. *Nature*, 518(7540):529–533.

Moore, A. W. (1990). Efficient memory-based learning for robot control. Technical report, University of Cambridge.

Munos, R., Stepleton, T., Harutyunyan, A., and Bellemare, M. (2016). Safe and efficient off-policy reinforcement learning. In *Advances in Neural Information Processing Systems*.

Nair, V. and Hinton, G. E. (2010). Rectified linear units improve restricted boltzmann machines. In *Proceedings of the International Conference on Machine Learning*.

Oliphant, T. E. (2006). *A guide to NumPy*, volume 1. Trelgol Publishing USA.

Oliphant, T. E. (2007). Python for scientific computing. *Computing in Science & Engineering*, 9(3):10–20.

Ollivier, Y. (2018). Approximate temporal difference learning is a gradient descent for reversible policies. *arXiv preprint arXiv:1805.00869*.

Oord, A. v. d., Li, Y., and Vinyals, O. (2018). Representation learning with contrastive predictive coding. *arXiv preprint arXiv:1807.03748*.

Osband, I., Aslanides, J., and Cassirer, A. (2018). Randomized prior functions for deep reinforcement learning. In *Advances in Neural Information Processing Systems*.

Paszke, A., Gross, S., Massa, F., Lerer, A., Bradbury, J., Chanan, G., Killeen, T., Lin, Z., Gimelshein, N., Antiga, L., Desmaison, A., Kopf, A., Yang, E., DeVito, Z., Raison, M., Tejani, A., Chilamkurthy, S., Steiner, B., Fang, L., Bai, J., and Chintala, S. (2019). Pytorch: An imperative style, high-performance deep learning library. In *Advances in Neural Information Processing Systems*.

Puterman, M. L. (1994). *Markov Decision Processes: Discrete Stochastic Dynamic Programming*. John Wiley & Sons.

Scherrer, B. (2010). Should one compute the temporal difference fix point or minimize the bellman residual? the unified oblique projection view. In *Proceedings of the International Conference on Machine Learning*.

Schwarzer, M., Anand, A., Goel, R., Hjelm, R. D., Courville, A., and Bachman, P. (2021). Data-efficient reinforcement learning with self-predictive representations. In *Proceedings of the International Conference on Learning Representations*.

Sutton, R., Precup, D., and Singh, S. (1999). Between MDPs and semi-MDPs: A framework for temporal abstraction in reinforcement learning. *Artificial Intelligence*, 112:181–211.

Sutton, R. S. (1988). Learning to predict by the methods of temporal differences. *Machine learning*, 3(1):9–44.

Sutton, R. S. and Barto, A. G. (1998). *Reinforcement learning: An Introduction*. MIT Press.

Sutton, R. S. and Barto, A. G. (2018). *Reinforcement learning: An Introduction*. MIT Press, 2nd edition.

Sutton, R. S., Mahmood, A. R., and White, M. (2016). An emphatic approach to the problem of off-policy temporal-difference learning. *Journal of Machine Learning Research*, 17(1):2603–2631.

Sutton, R. S., Modayil, J., Delp, M., Degris, T., Pilarski, P. M., White, A., and Precup, D. (2011). Horde: A scalable real-time architecture for learning knowledge from unsupervised sensorimotor interaction. In *Proceedings of the International Conference on Autonomous Agents and Multiagent Systems*.

Tang, C. (2019). Exponentially convergent stochastic k-pca without variance reduction. In *Advances in Neural Information Processing Systems*.

Tang, Y., Guo, Z. D., Richemond, P. H., Pires, B. Á., Chandak, Y., Munos, R., Rowland, M., Azar, M. G., Lan, C. L., Lyle, C., et al. (2023). Understanding self-predictive learning for reinforcement learning. *arXiv preprint arXiv:2212.03319*.

Thakoor, S., Rowland, M., Borsa, D., Dabney, W., Munos, R., and Barreto, A. (2022). Generalised policy improvement with geometric policy composition. In *Proceedings of the International Conference on Machine Learning*.

Touati, A. and Ollivier, Y. (2021). Learning one representation to optimize all rewards. In *Advances in Neural Information Processing Systems*.

Tsitsiklis, J. and Van Roy, B. (1996). Analysis of temporal-diffference learning with function approximation. In *Advances in Neural Information Processing Systems*.

Van Rossum, G. and Drake Jr, F. L. (1995). *Python reference manual*. Centrum voor Wiskunde en Informatica Amsterdam.

Walt, S. v. d., Colbert, S. C., and Varoquaux, G. (2011). The numpy array: a structure for efficient numerical computation. *Computing in science & engineering*, 13(2):22–30.

Watkins, C. J. and Dayan, P. (1992). Q-learning. *Machine learning*, 8:279–292.

Yu, H. and Bertsekas, D. P. (2009). Basis function adaptation methods for cost approximation in mdp. In *Proceedings of the IEEE Symposium on Adaptive Dynamic Programming and Reinforcement Learning*.

Zhang, S., Yao, H., and Whiteson, S. (2021). Breaking the deadly triad with a target network. In *Proceedings of the International Conference on Machine Learning*.

A. Additional Empirical Results

A.1. Additional details for Subsection 5.1

In this experiment, we selected a step size $\alpha = 0.08$ for all the algorithms. We also choose a uniform data distribution $\Xi = I/|\mathcal{S}|$ and a cumulant matrix $G = I$ for simplicity.

A.2. Additional details for Subsection 5.2

In this experiment, we use a step size $\alpha = 5e^{-3}$ and train the different learning rules for 500k steps with 3 seeds. We consider the transition matrices induced by an epsilon greedy policy on the four room domain (Sutton et al., 1999) with $\epsilon = 0.8$ and train the supervised and TD update rules as described in Subsection 5.1. We provide additionnal empirical results in Figure 7.
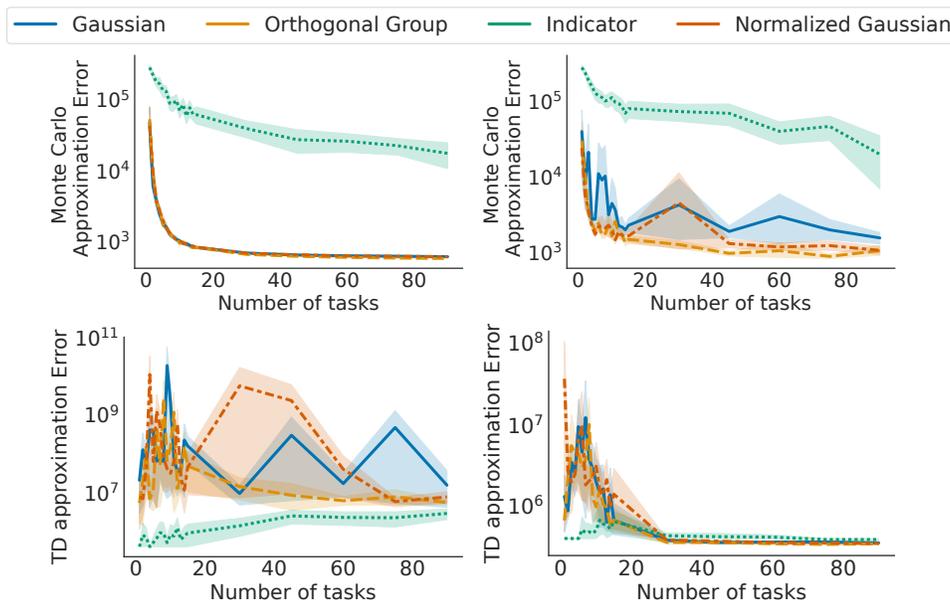
Figure 7: Monte Carlo and TD approximation errors after 5.10^5 training steps on the learning rules $\mathcal{L}_{\text{aux}}^{\text{MC}}$ (on the **left** column) and $\mathcal{L}_{\text{aux}}^{\text{TD}}$ (on the **right** column) in the four-room domain for different distributions of cumulant, averaged over 30 seeds, for $d = 5$. Shaded areas represent estimates of 95% confidence intervals.

A.3. Additional details for Subsection 5.3

Four Rooms is a tabular gridworld environment where the agent begins in a room in the top left corner and must navigate to the goal state in the lower right corner. The actions are up, down, left and right and have deterministic effects. The reward function is one upon transitioning into the goal state and zero otherwise.

Mountain Car is a two-dimensional continuous state environment where the agent must move an under-powered car from the bottom of a valley to a goal state at the top of the nearby hill. The agent observes the continuous-valued position and velocity of the car, and controls it with three discrete actions which apply positive, negative, and zero thrust to the car. In this sparse reward version of the domain the reward is one for reaching the goal and zero otherwise. In this domain, we compute the ExactSVD by first discretizing the state space into approximately 2000 states, and compute an approximate P^π by simulating transitions from uniformly random continuous states belonging to each discretized state.

In this evaluation we first pre-train a network representation offline with a large fixed dataset produced from following the uniform random policy. During offline pre-training the agent does not observe the reward, and instead learns action-value functions, GVFs, for each of several cumulant functions. After pre-training, the GVF head is removed and replaced with a single action-value function head. This network is then trained online with DQN on the true environmental reward. Note that we allow gradients to propagate into the network representation during online training.

In Four Rooms all methods use $k = 40$ cumulants and in Mountain Car all methods use $k = 80$ cumulants.

The inputs to the network were a one-hot encoding of the observation in the four-room domain and the usual position and velocity feature vector in Mountain car. The offline pre-training dataset contains 100000 and 200000 transitions for four-room and mountain car respectively. In both cases the dataset is generated and used to fill a (fixed) replay buffer, and then the agent is trained for 400000 updates (each update using a minibatch of 32 transitions sampled uniformly from the buffer/dataset). The learning rate for both offline and online training was the same as the standard DQN learning rate (0.00025), and similarly for the optimizer epsilon. The network architecture is a simple fully connected MLP with ReLU activations (Nair and Hinton, 2010) and two hidden layers of size 512 (first) and 256 (second), followed by a linear layer to give action-values.

We provide visualizations of the cumulants produced by each method and their corresponding value functions in Figure 8, Figure 9, Figure 11, Figure 12.

Figure 10 and Figure 13 also show the norm and srank of the representations being learned during offline pretraining.
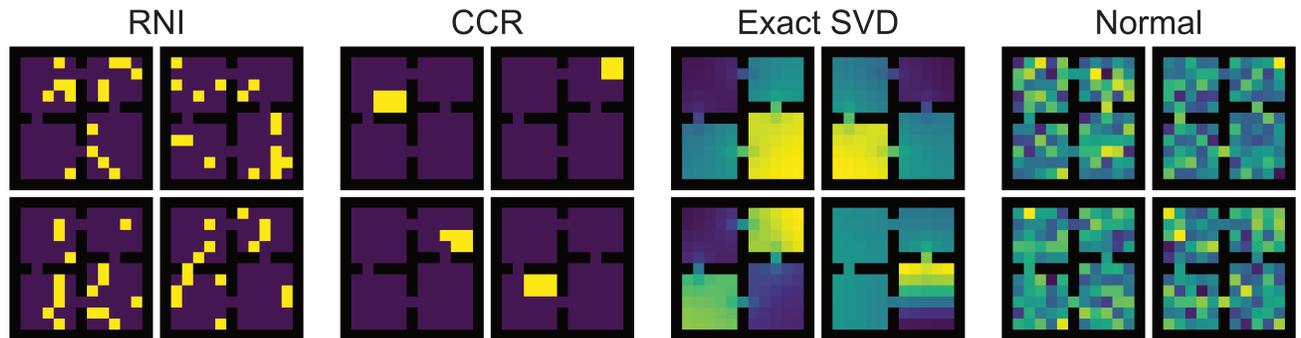
Figure 8: Examples of the learned cumulants produced during offline pre-training in FourRooms under the uniform random policy.
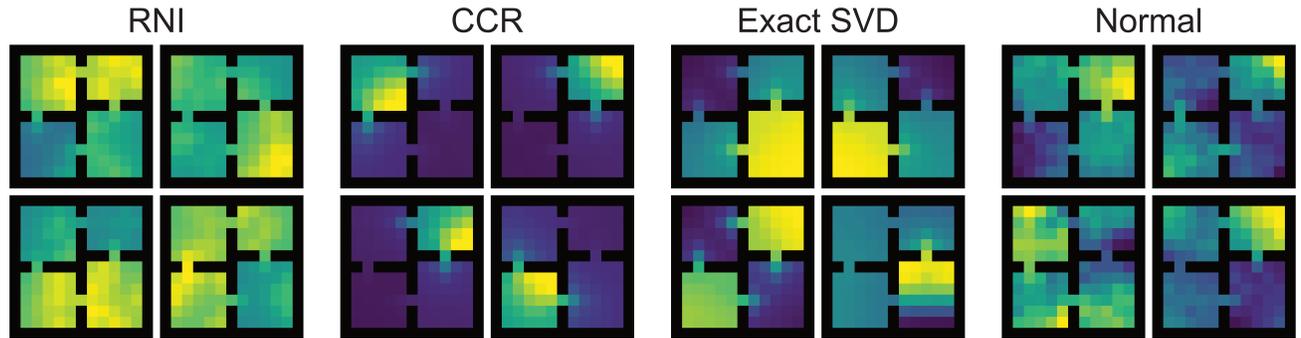
Figure 9: Examples of the learned (general) value functions produced during offline pre-training in FourRooms under the uniform random policy. In each case, the GVFs shown correspond to the value functions learned for the cumulants in Figure 8.
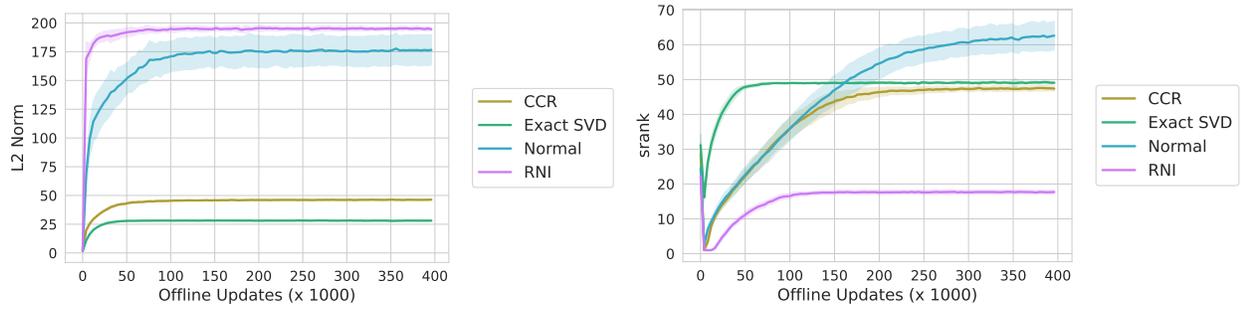
Figure 10: For the GVF-based representations during offline training in Four Rooms, their (**left**) L2 norm and (**right**) srank.
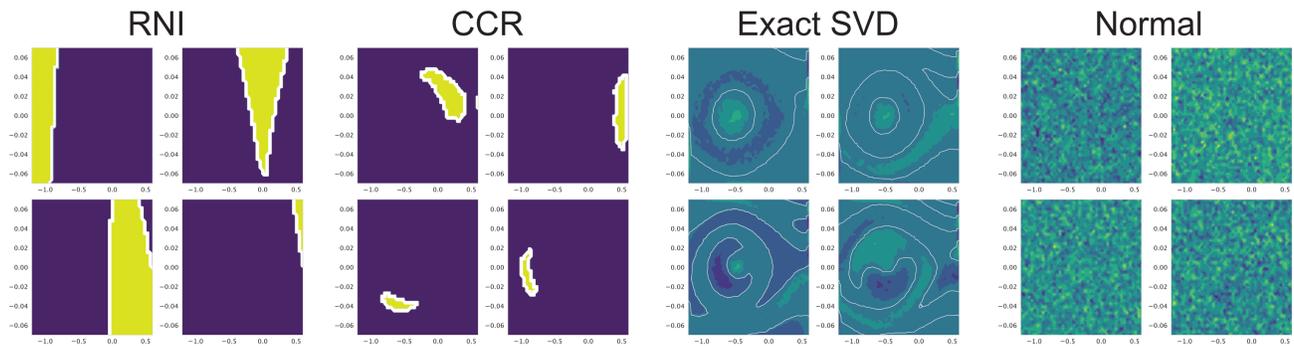

Figure 11: Examples of the learned cumulants produced during offline pre-training in sparse Mountain Car under the uniform random policy.
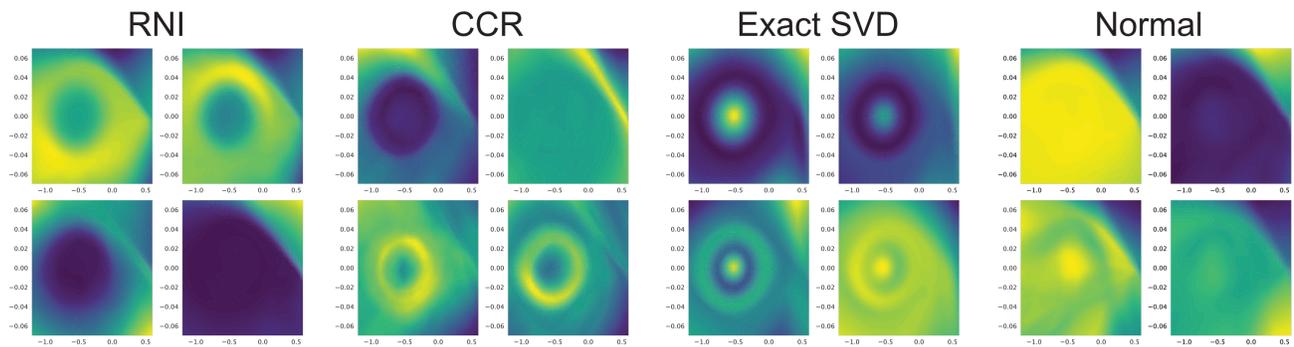

Figure 12: Examples of the learned (general) value functions produced during offline pre-training in sparse Mountain Car under the uniform random policy. In each case, the GVFs shown correspond to the value functions learned for the cumulants in Figure 11.
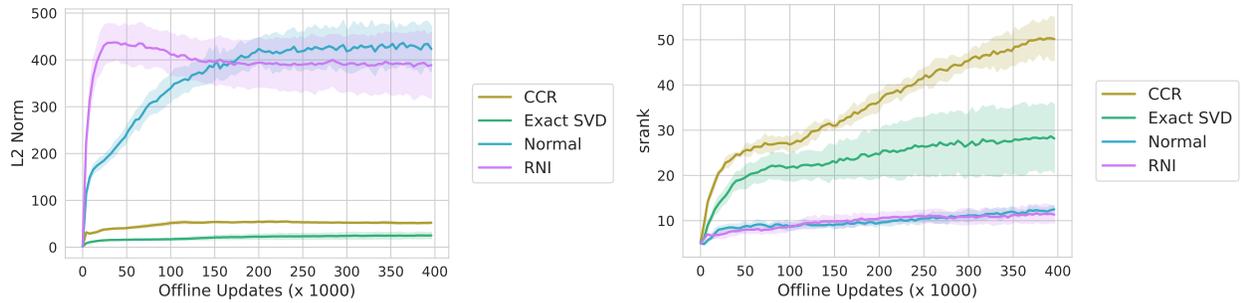
Figure 13: For the GVF-based representations during offline training in sparse Mountain Car, their (**left**) L2 norm and (**right**) srank.
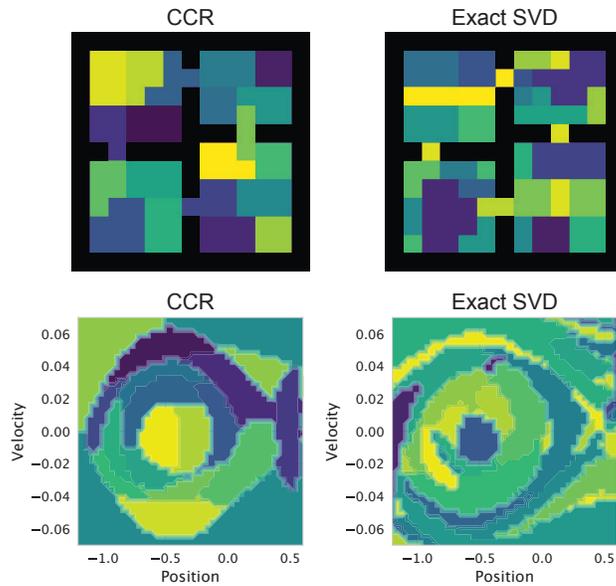
Figure 14: As CCR is effectively a clustering of states, we might ask in which states each cluster is active. We show an example of the maximally active cluster index for CCR (**left**) and Exact SVD (**right**) in the Four Rooms (**top**) and sparse Mountain Car (**bottom**) domains. These examples are for 20 cumulants setting.

B. Proofs for Section 2

Proposition 1 (Monte Carlo representations). *If* $\operatorname{rank}(\Psi^\pi) \geqslant d \geqslant 1$, *all representations spanning the top-d left singular vectors of Ψ^π with respect to the inner product $\langle x, y \rangle_\Xi$ are global minimizers of $\mathcal{L}_{\text{aux}}^{\text{MC}}$ and can be recovered by stochastic gradient descent.*

Proof. Let F_d denote the top d left singular vectors of Ψ.

$$\underset{\Phi \in \mathbb{R}^{S \times d}}{\arg\min} \min_{W \in \mathbb{R}^{d \times T}} \|\Xi^{1/2}(\Phi W - \Psi)\|_F^2 = \underset{\Phi \in \mathbb{R}^{S \times d}}{\arg\min} \|P_{\Xi^{1/2}\Phi}^\perp \Xi^{1/2} \Psi\|_F^2$$

$$= \{\Phi \in \mathbb{R}^{S \times d} \mid \exists M \in GL_d(\mathbb{R}), \Phi = F_d M\}$$

The problem on the left side is a bilinear optimization problem in the variables (Φ, W). Despite the non-convexity of this problem, it is now well known that these types of optimization problems can be efficiently solved using (noisy) gradient descent efficiently, i.e., with number of iterations scaling at most polynomially in all problem specific parameters (Ge et al., 2017; Jin et al., 2017).

$\square$

C. Proofs for Section 3

Throughout the appendix, we will use the notation $L := I - \gamma P^\pi$.

The beginning of this section is dedicated to proving the main result of Section 3, Theorem 1. Before that, we introduce the following necessary lemma.

Lemma 7. *Let $\Phi \in \mathbb{R}^{S \times d}$ and $\Psi \in \mathbb{R}^{S \times T}$. Let P_Φ be a (possibly oblique) projection onto $\operatorname{span}(\Phi)$. We have*

$$P_\Phi \Psi = \Psi \iff \operatorname{span}(\Psi) \subseteq \operatorname{span}(\Phi)$$

Proof. P_Φ can be written as $P_\Phi = \Phi(X^\top \Phi)^{-1} X^\top$ where $\Phi, X \in \mathbb{R}^{S \times d}$ and $X^\top \Phi \in \mathbb{R}^{d \times d}$ is invertible. Write $P_\Phi = \Phi Q$ with $Q = (X^\top \Phi)^{-1} X^\top$.

($\implies$) Suppose $\Psi \in \mathbb{R}^{S \times T}$ such that $P_\Phi \Psi = \Psi$. Then, $\Psi = \Phi(Q\Psi)$. Let $\omega \in \mathbb{R}^T$. $\Psi \omega = \Phi(Q\Psi)\omega$ so $\Psi \omega \in \operatorname{span}(\Phi)$ Hence $\operatorname{span}(\Psi) \subseteq \operatorname{span}(\Phi)$.

($\impliedby$) Suppose $\operatorname{span}(\Psi) \subseteq \operatorname{span}(\Phi)$. Denote (e_t) the standard basis. We have $P_\Phi \Psi = (\sum_t P_\Phi(\Psi e_t) e_t^\top)$. Note that $\Psi e_t \in \operatorname{span}(\Psi) \subseteq \operatorname{span}(\Phi)$. Hence, there exists $y_t \in \mathbb{R}^d$ such that $\Psi e_t = \Phi y_t$. Now, $P_\Phi \Psi = (\sum_t P_\Phi(\Phi y_t) e_t^\top) = (\sum_t \Phi(X^\top \Phi)^{-1} X^\top \Phi y_t e_t^\top) = (\sum_t \Phi y_t e_t^\top) = (\sum_t \Psi e_t e_t^\top) = \Psi$. $\square$

Lemma 1 (Critical representations for TD). *All full rank representations which are critical points to $\mathcal{L}_{\text{aux}}^{\text{TD}}$ span real invariant subspaces of $(I - \gamma P^\pi)^{-1} G G^\top \Xi$, that is $\operatorname{span}((I - \gamma P^\pi)^{-1} G G^\top \Xi \Phi) \subseteq \operatorname{span}(\Phi)$.*

Proof. Start with these equations.

$$\text{For a fixed } \Phi, \nabla_W \|(\Xi)^{\frac{1}{2}}(\Phi W - G - \gamma P^\pi \text{SG}[\Phi W])\|_F^2 = 2\Phi^\top \Xi(\Phi W - G - \gamma P^\pi \Phi W)$$

$$\text{For a fixed } W, \nabla_\Phi \|(\Xi)^{\frac{1}{2}}(\Phi W - G - \gamma P^\pi \text{SG}[\Phi W])\|_F^2 = 2\Xi(\Phi W - G - \gamma P^\pi \Phi W)W^\top$$

By Assumption 1, $\Phi^\top \Xi L \Phi$ is invertible for all full rank representations Φ. Hence, for a fixed full rank Φ,

$$\nabla_W \|(\Xi)^{\frac{1}{2}}(\Phi W - G - \gamma P^\pi \text{SG}[\Phi W])\|_F^2 = 0 \iff W_\Phi^* = (\Phi^\top \Xi L \Phi)^{-1} \Phi^\top \Xi G$$

Using the second fixed-point equation:

$$0 = (L\Phi W - G)W^\top \iff L\Phi W W^\top = G W^\top.$$

Now plugging in the expression for W_Φ^*,

$$L\Phi\left(\Phi^\mathsf{T}D_\pi L\Phi\right)^{-1}\Phi^\mathsf{T}D_\pi G\left(\left(\Phi^\mathsf{T}D_\pi L\Phi\right)^{-1}\Phi^\mathsf{T}D_\pi G\right)^\mathsf{T} = G\left(\left(\Phi^\mathsf{T}D_\pi L\Phi\right)^{-1}\Phi^\mathsf{T}D_\pi G\right)^\mathsf{T}$$

$$\Leftrightarrow L\Phi\left(\Phi^\mathsf{T}D_\pi L\Phi\right)^{-1}\Phi^\mathsf{T}D_\pi GG^\mathsf{T}D_\pi\Phi\left(\Phi^\mathsf{T}D_\pi L\Phi\right)^{-\mathsf{T}} = GG^\mathsf{T}D_\pi\Phi\left(\Phi^\mathsf{T}D_\pi L\Phi\right)^{-\mathsf{T}}$$

$$\Leftrightarrow \Phi\left(\Phi^\mathsf{T}D_\pi L\Phi\right)^{-1}\Phi^\mathsf{T}D_\pi GG^\mathsf{T}D_\pi\Phi = L^{-1}GG^\mathsf{T}D_\pi\Phi$$

$$\Leftrightarrow \Pi_{L^\mathsf{T}D_\pi\Phi}L^{-1}GG^\mathsf{T}D_\pi\Phi = L^{-1}GG^\mathsf{T}D_\pi\Phi$$

where $\Pi_X = \Phi(X^\mathsf{T}\Phi)^{-1}X^\mathsf{T}$ is the oblique projection onto $\mathrm{span}(\Phi)$ orthogonally to $\mathrm{span}(X)$. This is equivalent to $\Pi^\perp_{L^\mathsf{T}D_\pi\Phi}L^{-1}GG^\mathsf{T}D_\pi\Phi = 0$, which is equivalent to saying that $\mathrm{span}(\Phi)$ must be an *invariant subspace* of $L^{-1}GG^\mathsf{T}D_\pi$ by Lemma 7.

In other words, we have shown that all non-degenerate full-rank Φ which are critical points span invariant subspaces of $L^{-1}GG^\mathsf{T}D_\pi$. $\qquad\square$

Corollary 1. *If $G = I$ and $\Xi = I/S$, all full rank representations which are critical points to $\mathcal{L}_{\mathrm{aux}}^{\mathrm{TD}}$ span real invariant subspaces of the invariant subspaces of P^π.*

Proof. Let $G = I$ and $\Xi = I/|S|$. By Lemma 1, all full rank representations which are critical points of $\mathcal{L}_{\mathrm{aux}}^{\mathrm{TD}}$ span real invariant subspaces of $(I - \gamma P^\pi)^{-1}$.

Let Φ be a representation spanning an invariant subspace of $(I - \gamma P^\pi)^{-1}$. By definition, $\mathrm{span}((I - \gamma P^\pi)^{-1}\Phi) \subseteq \mathrm{span}(\Phi)$. Because $(I - \gamma P^\pi)$ is invertible, we have $\dim((I - \gamma P^\pi)^{-1}\Phi) = \dim(\Phi)$. Hence, we actually have $\mathrm{span}((I - \gamma P^\pi)^{-1}\Phi) = \mathrm{span}(\Phi)$. There exists $w_1, w_2 \in \mathbb{R}^d$ such that $\Phi w_1 = (I - \gamma P^\pi)^{-1}\Phi w_2$ so $(I - \gamma P^\pi)\Phi w_1 = \Phi w_2$. It follows that $\Phi\frac{(w_1 - w_2)}{\gamma} = P^\pi\Phi w_1$. Hence, $P^\pi\Phi w_1 \in \mathrm{span}(\Phi)$ and $\mathrm{span}(P^\pi\Phi) \subseteq \mathrm{span}(\Phi)$. We conclude that Φ spans an invariant subspace of P^π. $\qquad\square$

Theorem 1 (TD representations). *Assume P^π real diagonalisable, $G = I$ and a uniform distribution ξ over states. Let $(v_1, \ldots, v_S)$ denote the eigenvectors of P^π corresponding to the eigenvalues $(\lambda_1, \ldots, \lambda_S)$. Under the dynamics in Equation (2), all real invariant subspaces of dimension d are critical points, and any real non top-d invariant subspace $\Phi = (v_{i_1}, \ldots, v_{i_d})$ is unstable for gradient descent.*

Proof. Consider this objective:

$$\mathcal{L}(\Phi) = \frac{1}{2}\|(\Xi^{\frac{1}{2}})(\Phi W_{\Phi,G}^{\mathrm{TD}} - G - \gamma P^\pi\mathrm{SG}[\Phi W_{\Phi,G}^{\mathrm{TD}}])\|_F^2,$$

and $W_{\Phi,G}^{\mathrm{TD}} = \left(\Phi^\mathsf{T}\Xi L\Phi\right)^{-1}\Phi^\mathsf{T}\Xi G$ and define $L := I - \gamma P^\pi$. Observe that:

$$\text{For a fixed } W, \nabla_\Phi\|\Phi W - G - \gamma P^\pi\mathrm{SG}[\Phi W]\|_F^2 = 2\Xi(L\Phi W - G)(W)^\mathsf{T}$$

So now we consider the continuous time dynamics:

$$\frac{d}{dt}\Phi = -\nabla_\Phi\mathcal{L}(\Phi) := -F(\Phi), \tag{5}$$

where:

$$F(\Phi) := \Xi(L\Phi W_{\Phi,G}^{\mathrm{TD}} - G)(W_{\Phi,G}^{\mathrm{TD}})^\mathsf{T} = \Xi L(\Pi_{L^\mathsf{T}\Xi\Phi} - I)L^{-1}GG^\mathsf{T}\Xi\Phi(\Phi^\mathsf{T}\Xi L\Phi)^{-\mathsf{T}}$$

Consider the case $G = I$ and $\Xi = I/|\mathcal{S}|$.

The proof strategy consists in constructing an eigenvector $\Delta \in \mathbb{R}^{S \times d}$ of $\partial_\Phi F(\Phi)$ as a function of Φ, L, G such that $\partial_\Phi F(\Phi)[\Delta] = -\lambda\Delta$ for some $\mathrm{Re}(\lambda) > 0$. For every non top-d invariant subspace, we prove that the Jacobian of the dynamics $-F$ has a positive real part eigenvalue.

$$\partial_\Phi F(\Phi)[\Delta] = (L\Delta W_\Phi^* + L\Phi(dW_\Phi^*))(W_\Phi^*)^\mathsf{T} + (L\Phi W_\Phi^* - I)(dW_\Phi^*)^\mathsf{T}$$
$$\partial_\Phi W_\Phi^*[\Delta] = -(\Phi^\mathsf{T} L\Phi)^{-1}(\Delta^\mathsf{T} L\Phi + \Phi^\mathsf{T} L\Delta)(\Phi^\mathsf{T} L\Phi)^{-1}\Phi^\mathsf{T} + (\Phi^\mathsf{T} L\Phi)^{-1}\Delta^\mathsf{T}.$$

We also have the identity

$$W = (\Phi^\mathsf{T} L\Phi)^{-1}\Phi^\mathsf{T}.$$

Now, if it is the case that $\Delta^\mathsf{T}\Phi = 0$, then by the L-invariance of Φ, we also have that $\Delta^\mathsf{T} L\Phi = 0$, and hence:

$$W\Delta = 0, \quad WL^\mathsf{T}\Delta = 0.$$

Next, we start with the simplification:

$$\partial_\Phi W_\Phi^*[\Delta] = -(\Phi^\mathsf{T} L\Phi)^{-1}\Phi^\mathsf{T} L\Delta(\Phi^\mathsf{T} L\Phi)^{-1}\Phi^\mathsf{T} + (\Phi^\mathsf{T} L\Phi)^{-1}\Delta^\mathsf{T}$$
$$= -WL\Delta W + (\Phi^\mathsf{T} L\Phi)^{-1}\Delta^\mathsf{T}.$$

Using the shorthand $W = W_\Phi^*$ and the optimality condition $(L\Phi W - I)W^\mathsf{T} = 0$,

$$(L\Delta W + L\Phi(\partial W))W^\mathsf{T} = L\Delta WW^\mathsf{T} - L\Phi WL\Delta WW^\mathsf{T}$$
$$(L\Phi W - I)(\partial W)^\mathsf{T} = (L\Phi W - I)\Delta(\Phi^\mathsf{T} L\Phi)^{-\mathsf{T}} = -\Delta(\Phi^\mathsf{T} L\Phi)^{-\mathsf{T}}.$$

Therefore:

$$\partial_\Phi F(\Phi)[\Delta] = L\Delta WW^\mathsf{T} - L\Phi WL\Delta WW^\mathsf{T} - \Delta(\Phi^\mathsf{T} L\Phi)^{-\mathsf{T}}.$$

Furthermore, let us write $L\Phi = \Phi N$ for $N \in \mathbb{R}^{d\times d}$ with N invertible; this holds for some such N since Φ is L-invariant and rank d. With this notation, we see immediately that $L\Phi W = P_\Phi$, since:

$$\Phi^\mathsf{T} L\Phi = \Phi^\mathsf{T}\Phi N \implies W = (\Phi^\mathsf{T} L\Phi)^{-1}\Phi^\mathsf{T} = N^{-1}(\Phi^\mathsf{T}\Phi)^{-1}\Phi^\mathsf{T},$$

and therefore:

$$L\Phi W = \Phi NW = \Phi(\Phi^\mathsf{T}\Phi)^{-1}\Phi^\mathsf{T} = P_\Phi.$$

Hence:

$$\partial_\Phi F(\Phi)[\Delta] = P_\Phi^\perp L\Delta WW^\mathsf{T} - \Delta(\Phi^\mathsf{T} L\Phi)^{-\mathsf{T}}.$$

This is the starting point of our analysis. Let $(v_1, \ldots, v_S)$ denote the eigenvectors of P corresponding to $(\lambda_1, \ldots, \lambda_S)$. Let us choose $\Delta = P_\Phi^\perp v_i u^\mathsf{T}$. The identity $P_\Phi^\perp L\Delta = (1 - \gamma\lambda_i)\Delta$ yields that:

$$\partial_\Phi F(\Phi)[\Delta] = \Delta[(1 - \gamma\lambda_i)I - N]N^{-1}(\Phi^\mathsf{T}\Phi)^{-1}N^{-\mathsf{T}}.$$

Let $(v_1, \ldots, v_S)$ denote the eigenvectors of P corresponding to $(\lambda_1, \ldots, \lambda_S)$. Let the columns of Φ be $(v_{i_1}, \ldots, v_{i_d})$ with corresponding eigenvalues $(\lambda_{i_1}, \ldots, \lambda_{i_d})$. Then, we have the identity:

$$L\Phi = \Phi(I - \gamma\Lambda), \quad \Lambda = \text{diag}(\lambda_{i_1}, \ldots, \lambda_{i_d}).$$

Note that:

$$W = (I - \gamma\Lambda)^{-1}(\Phi^\mathsf{T}\Phi)^{-1}\Phi^\mathsf{T},$$
$$WW^\mathsf{T} = (I - \gamma\Lambda)^{-1}(\Phi^\mathsf{T}\Phi)^{-1}(I - \gamma\Lambda)^{-1},$$
$$L\Phi W = P_\Phi,$$

so we have:

$$\partial_\Phi F(\Phi)[\Delta] = P_\Phi^\perp L\Delta WW^\mathsf{T} - \Delta(\Phi^\mathsf{T}\Phi)^{-1}(I - \gamma\Lambda)^{-1}.$$

Next, we will choose $\Delta = P_\Phi^\perp v_i u^\mathsf{T}$, with the index i and vector u to be specified. Note that if we want $\Delta \neq 0$ we are constrained to choosing $i \notin \{i_1, \ldots, i_d\}$.

With this choice:

$$P_\Phi^\perp L\Delta = P_\Phi^\perp[(1 - \gamma\lambda_i)v_i u^\mathsf{T} - LP_\Phi v_i u^\mathsf{T}] = (1 - \gamma\lambda_i)\Delta,$$

where the last equality holds since by the L-invariance of Φ, we have that $P_\Phi^\perp LP_\Phi = 0$. Hence:

$$\begin{aligned}\partial_\Phi F(\Phi)[\Delta] &= (1 - \gamma\lambda_i)\Delta(I - \gamma\Lambda)^{-1}(\Phi^\mathsf{T}\Phi)^{-1}(I - \gamma\Lambda)^{-1} - \Delta(\Phi^\mathsf{T}\Phi)^{-1}(I - \gamma\Lambda)^{-1}. \\ &= -\gamma\Delta(\lambda_i I - \Lambda)(I - \gamma\Lambda)^{-1}(\Phi^\mathsf{T}\Phi)^{-1}(I - \gamma\Lambda)^{-1}.\end{aligned}$$

So, we just need to choose u to be a left eigenvector of the matrix $(\lambda_i I - \Lambda)(I - \gamma\Lambda)^{-1}(\Phi^\mathsf{T}\Phi)^{-1}(I - \gamma\Lambda)^{-1}$, associated with the largest eigenvalue. Thus, it remains to show that this matrix has at least one positive eigenvalue. By using the fact that the eigenvalues of size conforming matrices AB equals the eigenvalues of BA, the eigenvalues of this matrix are:

$$\begin{aligned}&\mathrm{eig}((\lambda_i I - \Lambda)(I - \gamma\Lambda)^{-1}(\Phi^\mathsf{T}\Phi)^{-1}(I - \gamma\Lambda)^{-1}) \\ &= \mathrm{eig}((I - \gamma\Lambda)^{-1}(\lambda_i I - \Lambda)(I - \gamma\Lambda)^{-1}(\Phi^\mathsf{T}\Phi)^{-1}) \\ &= \mathrm{eig}((\Phi^\mathsf{T}\Phi)^{-1/2}(I - \gamma\Lambda)^{-1}(\lambda_i I - \Lambda)(I - \gamma\Lambda)^{-1}(\Phi^\mathsf{T}\Phi)^{-1/2}).\end{aligned}$$

Now, we need an auxiliary lemma.

Proposition 4. *Let A, B be symmetric matrices, with B invertible. We have that:*

$$\lambda_{\max}(BAB) \geqslant \frac{\lambda_{\max}(A)}{\lambda_{\max}(B^{-2})}.$$

Proof. Let q be the unit eigenvector associated with the largest eigenvalue of A. Since BAB is symmetric, we can use the variational characterization of the largest eigenvalue to show:

$$\begin{aligned}\lambda_{\max}(BAB) &= \sup_{\|v\|=1} v^\mathsf{T} BABv \\ &\geqslant \frac{q^\mathsf{T} Aq}{\|B^{-1}q\|^2} && \text{choosing } v = \frac{B^{-1}q}{\|B^{-1}q\|} \\ &= \frac{\lambda_{\max}(A)}{\|B^{-1}q\|^2} \\ &\geqslant \frac{\lambda_{\max}(A)}{\lambda_{\max}(B^{-2})} && \text{since } \|B^{-1}q\| \leqslant \|B^{-1}\|_{\mathrm{op}}.\end{aligned}$$

$\square$

With this proposition, we can conclude the proof. In particular, since we assume that Φ contains at least one eigenvector associated with $\lambda_{d+1}, \ldots, \lambda_S$, then as long as we choose the index i of v in the following set $[d] \cap \{i_1, \ldots, i_d\}^c$ (where the set complementation is done w.r.t. $[S]$), then we will satisfy both (a) $\Delta \neq 0$ and (b) there is at least one diagonal entry in $\lambda_i I - \Lambda$ which is positive (this is where the strict gap assumption $\lambda_d > \lambda_{d+1}$ enters). Hence, we have that $\lambda_{\max}((I - \gamma\Lambda)^{-1}(\lambda_i I - \Lambda)(I - \gamma\Lambda)^{-1}) > 0$, which concludes the proof.

$\square$

Proposition 2 (Residual representations). *Let $d \in \{1, ..., S\}$ and F_d be the top d left singular vectors of G with respect to the inner product $\langle x, y\rangle_\Xi = y^\mathsf{T}\Xi x$, for all $x, y \in \mathbb{R}^S$. All representations spanning $(I - \gamma P^\pi)^{-1} F_d$ are global minimizers of $\mathcal{L}_{\mathrm{aux}}^{\mathrm{res}}$ and can be recovered by stochastic gradient descent.*

Proof. We can write the loss function to be minimized as

$$J(\Phi) = \min_{W \in \mathbb{R}^{d \times T}} \|\Xi^{1/2}(\Phi W - (G + \gamma P^\pi \Phi W))\|_F^2$$

$$= \min_{W \in \mathbb{R}^{d \times T}} \|\Xi^{1/2}(\Phi W - \gamma P^\pi \Phi W - G)\|_F^2$$

$$= \min_{W \in \mathbb{R}^{d \times T}} \|\Xi^{1/2}((I - \gamma P^\pi)\Phi W - G)\|_F^2$$

Now,

$$\arg\min_{\Phi \in \mathbb{R}^{S \times d}} \min_{W \in \mathbb{R}^{d \times T}} \|\Xi^{1/2}((I - \gamma P^\pi)\Phi W - G)\|_F^2 = \arg\min_{\Phi \in \mathbb{R}^{S \times d}} \|P_{\Xi^{1/2}(I - \gamma P^\pi)\Phi}^\perp \Xi^{1/2} G\|_F^2$$

$$= \{\Phi \in \mathbb{R}^{S \times d} \mid \Phi = (I - \gamma P^\pi)^{-1} F_d M, M \in GL_d(\mathbb{R})\}$$

This set of representations can be recovered by stochastic gradient descent efficiently, i.e., with number of SGD iterations scaling at most polynomially in all problem specific parameters (Ge et al., 2017; Jin et al., 2017) in the context of SGD. $\square$

Corollary 2 (Symmetric transition matrices)**.** *If a cumulant matrix $G \in \mathbb{R}^{S \times T}$ (with $T \geqslant S$) has unit-norm, orthogonal columns (e.g. $G = I$), the representations learnt from the supervised objective $\mathcal{L}_{\mathrm{aux}}^{\mathrm{MC}}$ and the TD update rule $\mathcal{L}_{\mathrm{aux}}^{\mathrm{TD}}$ are the same for symmetric transition matrices P^π under a uniform state distribution ξ.*

Proof. Assume that P^π is symmetric so that L and L^{-1} are also symmetric.

By Proposition 1, running SGD on the supervised objective $\mathcal{L}_{\mathrm{aux}}^{\mathrm{MC}}$ using $\Psi = L^{-1}G$ as targets results in a representation spanning the top-d left singular vectors of $L^{-1}G$ which are the same as the top-d left singular vectors of L^{-1}.

By assumption G is orthogonal, hence $GG^\mathsf{T} = I$. Because $L^{-1}GG^\mathsf{T}$ is symmetric, all its eigenvalues are real. By Theorem 1, running gradient descent on $\mathcal{L}_{\mathrm{aux}}^{\mathrm{TD}}$ using G as the cumulant matrix converges to the top-d eigenvectors of $L^{-1}GG^\mathsf{T} = L^{-1}$. Indeed, the subspaces given by the span of the right eigenvectors of L^{-1} are the only L^{-1}-invariant subspaces. These eigenvectors are also the singular vectors of L^{-1} as this matrix is symmetric.

Because P is a row stochastic matrix, we have that the spectral radius of P satisfies $\rho(P) = 1$, and therefore $\lambda(P) \subseteq [-1, 1]$. Hence:

$$\frac{1}{1 - \gamma\lambda} \in [1/(1 + \gamma), 1/(1 - \gamma)].$$

Hence, the eigenvalues of L^{-1} are positive. Because L^{-1} is symmetric, the singular values of L^{-1} are exactly its eigenvalues. Hence, the top-d eigenvectors are the top-d singular vectors and the conclusion follows. $\square$

D. Proofs for Section 4

Lemma 2. *A representation Φ_{TD}^* is l_1-ball optimal for TD learning iff it is a solution of the following optimization problem.*

$$\Phi_{\mathrm{TD}}^* \in \arg\min_\Phi \left\| \Xi^{1/2}(\Phi W_{\Phi,I}^{\mathrm{TD}} - (I - \gamma P^\pi)^{-1}) \right\|_F^2.$$

Proof. By definition, a representation is enough for TD learning when it is a minimizer of Equation (3), that is,

$$\Phi_{\mathrm{TD}}^* \in \arg\min_{\Phi \in \mathbb{R}^{S \times d}} \mathbb{E}_{r_\pi} \|\Phi w_\Phi^{\mathrm{TD}} - V^\pi\|_\xi^2, \tag{6}$$

where the expectation is over the reward functions r_π sampled uniformly over the l_1 ball $\|r_\pi\|_1^2 \leqslant 1$ and

$$w_\Phi^{\mathrm{TD}} = \left(\Phi^\mathsf{T} \Xi (I - \gamma P^\pi)\Phi\right)^{-1} \Phi^\mathsf{T} \Xi r_\pi.$$

Write $P^\perp_{L^\intercal \Xi \Phi} = I - P_{L^\intercal \Xi \Phi}$ and $P_X = \Phi(X^\intercal \Phi)^{-1} X^\intercal$ the oblique projection onto $\mathrm{span}(\Phi)$ orthogonally to $\mathrm{span}(X)$. We have

$$
\begin{aligned}
\mathbb{E}_{\|r\|_1^2 \leqslant 1} \|\Phi w_\Phi^{\mathrm{TD}} - V^\pi\|_\xi^2 &= \mathbb{E}_{\|r\|_1^2 \leqslant 1} \|\Xi^{1/2} P^\perp_{L^\intercal \Xi \Phi}(I - \gamma P^\pi)^{-1} r\|_2^2 \\
&= \mathbb{E}_{\|r\|_1^2 \leqslant 1} \|\Xi^{1/2} P^\perp_{L^\intercal \Xi \Phi}(I - \gamma P^\pi)^{-1} r\|_2^2 \\
&= \mathbb{E}_{\|r\|_1^2 \leqslant 1} \mathrm{tr}(r^\top L^{-\top}(P^\perp_{L^\intercal \Xi \Phi})^\top \Xi P^\perp_{L^\intercal \Xi \Phi} L^{-1} r) \\
&= \mathrm{tr}(L^{-\top}(P^\perp_{L^\intercal \Xi \Phi})^\top \Xi P^\perp_{L^\intercal \Xi \Phi} L^{-1} \mathbb{E}(rr^\top)) \\
&\propto \|\Xi^{1/2} P^\perp_{L^\intercal \Xi \Phi} L^{-1}\|_F^2 \text{ because } r \text{ is sampled from an isotropic distribution} \\
&\propto \left\|\Xi^{1/2}(\Phi W^{\mathrm{TD}}_{\Phi,I} - (I - \gamma P^\pi)^{-1})\right\|_F^2
\end{aligned}
$$

$\square$

Lemma 3. *A representation Φ^*_{MC} is l_1-ball optimal for batch Monte Carlo policy evaluation if its column space spans the top-d left singular vectors (with respect to the inner product $\langle x, y \rangle_\Xi$) of $(I - \gamma P^\pi)^{-1}$.*

Proof. We have

$$
\begin{aligned}
\mathbb{E}_{\|r\|_1^2 \leqslant 1} \|\hat{V}^{\mathrm{MC}} - V^\pi\|_\xi^2 &= \mathbb{E}_{\|r\|_1^2 \leqslant 1} \|P^\perp_{\Xi^{1/2}\Phi} \Xi^{1/2}(I - \gamma P^\pi)^{-1} r\|_2^2 \\
&= \mathbb{E}_{\|r\|_1^2 \leqslant 1} \mathrm{tr}(r^\top L^{-\top} \Xi^{1/2} P^\perp_{\Xi^{1/2}\Phi} \Xi^{1/2} L^{-1} r) \\
&= \mathrm{tr}(L^{-\top} \Xi^{1/2} P^\perp_{\Xi^{1/2}\Phi} \Xi^{1/2} L^{-1} \mathbb{E}(rr^\top)) \\
&= \|P^\perp_{\Xi^{1/2}\Phi} \Xi^{1/2} L^{-1}\|_F^2
\end{aligned}
$$

Write $(I - \gamma P^\pi)^{-1} = F\Sigma B^\top$ the weighted SVD of $(I - \gamma P^\pi)^{-1}$ where $F \in \mathbb{R}^{S \times S}$ such that $F^\intercal \Xi F = I$ and $B \in \mathbb{R}^{S \times S}$ such that $B^\intercal B = I$. Write F_d the top-d left singular vectors corresponding to the top-d singular values on the diagonal of Σ. By definition, an l_1-ball optimal representation is solution to the following optimization problem

$$
\begin{aligned}
\arg\min_{\Phi \in \mathbb{R}^{S \times d}} \mathbb{E}_{\|r\|_1^2 \leqslant 1} \|\hat{V}^{\mathrm{MC}} - V^\pi\|_\xi^2 &= \arg\min_{\Phi \in \mathbb{R}^{S \times d}} \|P^\perp_{\Xi^{1/2}\Phi} \Xi^{1/2} L^{-1}\|_F^2 \\
&= \arg\min_{\Phi \in \mathbb{R}^{S \times d}} \|P^\perp_{\Xi^{1/2}\Phi} \Xi^{1/2} F\Sigma B^\top\|_F^2
\end{aligned}
$$

By the Eckart-Young theorem, $\|P^\perp_{F_d} \Xi^{1/2} F\Sigma B^T\|_F^2 \leqslant \|P^\perp_\Phi \Xi^{1/2} F\Sigma B^T\|_F^2$. Hence, the set of optimal representations is $\{F_d M, M \in GL_d(\mathbb{R})\}$. $\square$

Lemma 8. *Write $F_d \Sigma_d B_d^\top$ the truncated weighted SVD of the successor representation $(I - \gamma P^\pi)^{-1}$. A representation is l_1-ball optimal for residual policy evaluation if its column space spans $F_d \Sigma_d$.*

Proof. Write $(I - \gamma P^\pi)^{-1} = F\Sigma B^\intercal$ the weighted SVD of $(I - \gamma P^\pi)^{-1}$ where $F \in \mathbb{R}^{S \times S}$ such that $F^\intercal \Xi F = I$ and $B \in \mathbb{R}^{S \times S}$ such that $B^\intercal B = I$. Write F_d the top-d left singular vectors corresponding to the top-d singular values on the diagonal of Σ. For a fixed $\Phi \in \mathbb{R}^{S \times d}$, the solution of $\min_{w \in \mathbb{R}^d} \|\Xi^{1/2}(\Phi w - (r_\pi + \gamma P^\pi \Phi w))\|_F^2$ is the Bellman residual minimizing approximation (Lagoudakis and Parr, 2003) and is given by

$$
w^{\mathrm{res}}_\Phi = \left((\Phi - \gamma P^\pi \Phi)^\intercal \Xi (\Phi - \gamma P^\pi \Phi)\right)^{-1} (\Phi - \gamma P^\pi \Phi)^\intercal \Xi r_\pi.
$$

Hence, the value approximant can be expressed by means of an orthogonal projection matrix as follows

$$
\Phi w^{\mathrm{res}}_\Phi = (I - \gamma P^\pi)^{-1} \Xi^{-1/2} P_{\Xi^{1/2}(I - \gamma P^\pi)\Phi} \Xi^{1/2} r_\pi
$$

where $P_X = X(X^\mathsf{T}X)^{-1}X^T$ denotes an orthogonal projection. By definition, a representation l_1-ball optimal for residual policy evaluation is solution to the following optimization problem

$$\underset{\Phi \in \mathbb{R}^{S \times d}}{\arg \min} \mathbb{E}_{\|r\|_1^2 \leqslant 1} \|\hat{V}^{\text{res}} - V^\pi\|_\xi^2 = \underset{\Phi \in \mathbb{R}^{S \times d}}{\arg \min} \|\Xi^{1/2}(I-\gamma P^\pi)^{-1}\Xi^{-1/2}P_{\Xi^{1/2}(I-\gamma P^\pi)\Phi}\Xi^{1/2}r_\pi - \Xi^{1/2}(I-\gamma P^\pi)^{-1}r_\pi\|_F^2$$

$$= \underset{\Phi \in \mathbb{R}^{S \times d}}{\arg \min} \|\Xi^{1/2}(I-\gamma P^\pi)^{-1}\Xi^{-1/2}P_{\Xi^{1/2}(I-\gamma P^\pi)\Phi}\Xi^{1/2} - \Xi^{1/2}(I-\gamma P^\pi)^{-1}\|_F^2$$

$$= \underset{\Phi \in \mathbb{R}^{S \times d}}{\arg \min} \|\Xi^{1/2}(I-\gamma P^\pi)^{-1}P^\perp_{\Xi^{1/2}(I-\gamma P^\pi)\Phi}\|_F^2$$

Using an oblique projection,

$$\Phi w_\Phi^{\text{res}} = (I-\gamma P^\pi)^{-1}\Xi^{-1/2}P_{\Xi^{1/2}(I-\gamma P^\pi)\Phi}\Xi^{1/2}r_\pi$$

$$\underset{\Phi \in \mathbb{R}^{S \times d}}{\arg \min} \mathbb{E}_{\|r\|_1^2 \leqslant 1} \|\hat{V}^{\text{res}} - V^\pi\|_\xi^2 = \underset{\Phi \in \mathbb{R}^{S \times d}}{\arg \min} \|\Xi^{1/2}(I-\gamma P^\pi)^{-1}\Xi^{-1/2}P_{\Xi^{1/2}(I-\gamma P^\pi)\Phi}\Xi^{1/2}r_\pi - \Xi^{1/2}(I-\gamma P^\pi)^{-1}r_\pi\|_F^2$$

$$= \underset{\Phi \in \mathbb{R}^{S \times d}}{\arg \min} \|\Xi^{1/2}(I-\gamma P^\pi)^{-1}\Xi^{-1/2}P_{\Xi^{1/2}(I-\gamma P^\pi)\Phi}\Xi^{1/2} - \Xi^{1/2}(I-\gamma P^\pi)^{-1}\|_F^2$$

$$= \underset{\Phi \in \mathbb{R}^{S \times d}}{\arg \min} \|\Xi^{1/2}(I-\gamma P^\pi)^{-1}P^\perp_{\Xi^{1/2}(I-\gamma P^\pi)\Phi}\|_F^2$$

$$L^{-1} = U\Sigma V^\mathsf{T}$$

$L^{-1}\times$ the top d right singular vectors of $(I-\gamma P^\pi)^{-1}$ is a solution. Let U_d, Σ_d, V_d correspond to the top d svals. Lets say that U_d is $S \times d$, Σ_d is square, and V_d is also $S \times d$. What is $V^\mathsf{T}V_d = \begin{bmatrix} I_d \\ 0 \end{bmatrix}$.

We want $L\Phi = V_d$ so $\Phi = L^{-1}V_d = U\Sigma V^\mathsf{T}V_d = U_d\Sigma_d$. If $L\Phi = V_d$, then $P^\perp_{L\Phi} = P^\perp_{V_d}$, so $L^{-1}P^\perp_{V_d} = U_d^\perp\Sigma_d^\perp(V_d^\perp)^\mathsf{T}$, so the objective is now sum of the last $(S-d)$ singular values squared.

$\square$

E. Proofs for Subsection 4.1

Lemma 4. *Denote B_T the top-T right singular vectors of the SR and $\mathcal{O}(T,S)$ the set of orthogonal matrices in $\mathbb{R}^{T \times S}$. Training auxiliary tasks in a MC way with any G from the set $\{G \in \mathbb{R}^{S \times T} | \exists M \in \mathcal{O}(T,S), G = B_T M\}$ results in an l_1-ball optimal representation for batch Monte Carlo.*

Proof. By Lemma 3, a representation is l_1-ball optimal for batch Monte Carlo policy evaluation if it spans the top-d left singular vectors of the successor representation.

Let $G \in \mathbb{R}^{S \times T}$ be a cumulant matrix.

$$\mathcal{L}_{\text{aux}}^{\text{SL}}(\Phi) = \min_{W \in \mathbb{R}^{d \times S}} \|(\Phi W - (I-\gamma P^\pi)^{-1}G)\|_F^2$$

By Proposition 1, we know that training on such a loss with $G = I$ results in a representation spanning the same subspace as the left singular vectors of the SR, that is $\{\Phi \in \mathbb{R}^{S \times d} \mid \exists M \in GL_d(\mathbb{R}), \Phi = F_d M\}$ where F_d are the left singular vectors of the SR. We note that there is not a unique matrix G resulting into a representation spanning that subspace. In particular, training with any of the matrices from the set of cumulant matrices $\mathcal{G}(G) = \{G' \in \mathbb{R}^{S \times T} | \exists M \in \mathcal{O}(T,S), G' = GM\}$ results in the same representation, where $\mathcal{O}(T,S)$ denotes the set of orthogonal matrices in $\mathbb{R}^{T \times S}$ (rows have l2 norm 1).

We are interested in finding a cumulant matrix $G \in \mathbb{R}^{S \times T}$ with $T < S$ such that training the Monte Carlo loss $\mathcal{L}_{\text{aux}}^{\text{MC}}$ results in a representation spanning the top-d left singular vectors of the successor representation.

Denote B_T the top T right singular vectors of the SR. Then the set $\mathcal{G}(B_T)$ satisfies the requirement.

In particular, this finding is consistent in the case where $S = T$ because $\mathcal{G}(B_S) = \{G' \in \mathbb{R}^{S \times T} | \exists M \in \mathcal{O}(T), G' = B_S M\} = \mathcal{G}(I_S)$.

Indeed, let $G' \in \mathcal{G}(B_S)$. There exists $M \in \mathcal{O}(S)$ such that $G' = B_S M = I_S(B_S M)$. Because $B_S M \in \mathcal{O}(S)$, we have $G' \in \mathcal{G}(I_S)$. Hence $\mathcal{G}(B_S) \subset \mathcal{G}(I_S)$.

Let $G' \in \mathcal{G}(I_S)$. There exists $M \in \mathcal{O}(S)$ such that $G' = I_S M = (B_S B_S^\mathsf{T})M = B_S(B_S^\mathsf{T} M)$. Because $B_S^\mathsf{T} M \in \mathcal{O}(S)$, we have $G' \in \mathcal{G}(B_S)$. Hence $\mathcal{G}(I_S) \subset \mathcal{G}(B_S)$.

As a conclusion, we have $\mathcal{G}(I_S) = \mathcal{G}(B_S)$. $\qquad\square$

Lemma 5. *Let $\{\Phi_\omega\}$ be the set of rotating representations from Figure 2 learnt by TD learning with $G = I$ and $d = 2$. All these representations are equally good for learning the main value function by TD learning, that is $\forall \omega \in [0, 1]$,*

$$\mathbb{E}_{\|r\|_2^2 < 1} \left\| \Phi_\omega w_{\Phi_\omega}^{\mathrm{TD}} - V^\pi \right\|_F^2$$

is constant and independent of ω.

Proof. Let's start by considering the case of the three-state circular example. We consider an orthogonal basis for the invariant subspaces of Φ. By definition, $P^\pi e_1 = e_1, P^\pi[e_2, e_3] = [e_2, e_3]\Lambda$ so $Le_1 = (1 - \gamma)e_1$ and $L[e_2, e_3] = (I - \gamma P)[e_2, e_3] = [e_2, e_3] - \gamma[e_2, e_3]\Lambda = [e_2, e_3](I - \gamma\Lambda)$.

Assume that there exists $\omega \in [0, 1]$ such that the representation is $\Phi = [e_1, \omega e_2 + (1 - \omega)e_3] = [e_1, e_2, e_3]\Omega$ with
$\Omega = \begin{bmatrix} 1 & 0 \\ 0 & \omega \\ 0 & (1-\omega) \end{bmatrix}$. $L\Phi = [(1 - \gamma)e_1, [e_2, e_3](I - \gamma\Lambda)]\Omega$. Hence, we have $L\Phi = [e_1, e_2, e_3]\begin{bmatrix} 1 - \gamma & 0 \\ 0 & I - \gamma\Lambda \end{bmatrix}\Omega$

and $\Phi^\mathsf{T} L\Phi = \Omega^\mathsf{T}[e_1, e_2, e_3]^\mathsf{T}[e_1, e_2, e_3]\begin{bmatrix} 1 - \gamma & 0 \\ 0 & I - \gamma\Lambda \end{bmatrix}\Omega = \Omega^\mathsf{T}\begin{bmatrix} 1 - \gamma & 0 \\ 0 & I - \gamma\Lambda \end{bmatrix}\Omega$. Hence, $(\Phi^\mathsf{T} L\Phi)^{-1} = \begin{bmatrix} (1-\gamma)^{-1} & 0 \\ 0 & (u^\mathsf{T}(I - \gamma\Lambda)u)^{-1} \end{bmatrix}$ with $u = (w, (1 - w))^\mathsf{T}$. Note that $u^\mathsf{T}(I - \gamma\Lambda)u = \omega^2\lambda_{1,1} + (1 - \omega)^2\lambda_{1,1}$

The TD value function is given by $\hat{V}^{\mathrm{TD}} = \Phi(\Phi^\mathsf{T} L\Phi)^{-1}\Phi^\mathsf{T}$

$$\begin{aligned}
\hat{V}^{\mathrm{TD}} &= [e_1, e_2, e_3]\Omega\begin{bmatrix} (1-\gamma)^{-1} & 0 \\ 0 & (u^\mathsf{T}(I - \gamma\Lambda)u)^{-1} \end{bmatrix}\Omega^\mathsf{T}[e_1, e_2, e_3]^\mathsf{T} \\
&= [e_1, e_2, e_3]\begin{bmatrix} (1-\gamma)^{-1} & 0 \\ 0 & u(u^\mathsf{T}(I - \gamma\Lambda)u)^{-1}u^\mathsf{T} \end{bmatrix}[e_1, e_2, e_3]^\mathsf{T} \\
&= \frac{1/(1-\gamma)e_1 e_1^\mathsf{T} + \omega^2 e_2 e_2^\mathsf{T} + \omega(1-\omega)e_3 e_2^\mathsf{T} + \omega(1-\omega)e_2 e_3^\mathsf{T} + (1-\omega)^2 e_3 e_3^\mathsf{T}}{\omega^2\lambda_{1,1} + (1-\omega)^2\lambda_{1,1}}
\end{aligned}$$

Now $\|\Phi(\Phi^\mathsf{T} L\Phi)^{-1}\Phi^\mathsf{T} - V^\pi\|_F^2$ is independent of ω. $\qquad\square$

Lemma 6. *The set of cumulant matrices $G \in \mathbb{R}^{S \times T}$ that preserve the top-T invariant subspaces of the successor representation by TD learning are the top-T orthogonal invariant subspaces of $(I - \gamma P^\pi)^{-1}$, that is satisfying $G^\top G = I$ by orthogonality and $(I - \gamma P^\pi)^{-1}G \subseteq G$ by the invariance property.*

Proof. Let $\Phi \in \mathbb{R}^{S \times d}$ spanning an invariant subspace of L^{-1}. By definition, there exists a block diagonal matrix $J_\Phi \in \mathbb{R}^{d \times d}$ such that $L^{-1}\Phi = \Phi J_\Phi$. Let $G \in O(S, T)$ spanning the top T invariant subspaces of L^{-1}. By definition, there exists a block diagonal matrix $J_G \in \mathbb{R}^{d \times d}$ such that $L^{-1}G = GJ_G$. Hencer, we have

$$\begin{aligned}
(L^{-1}GG^\mathsf{T})\Phi &= (L^{-1}G)G^\mathsf{T}\Phi \\
&= GJ_T G^\mathsf{T}\Phi \\
&= (\Phi J_\Phi) \text{ by orthonormality}
\end{aligned}$$

Then, Φ is an invariant subspace of $L^{-1}GG^\top$. $\qquad\square$

Lemma 6. *The set of cumulant matrices $G \in \mathbb{R}^{S \times T}$ that preserve the top-T invariant subspaces of the successor representation by TD learning are the top-T orthogonal invariant subspaces of $(I - \gamma P^\pi)^{-1}$, that is satisfying $G^\top G = I$ by orthogonality and $(I - \gamma P^\pi)^{-1}G \subseteq G$ by the invariance property.*

Proof. Let $\Phi \in \mathbb{R}^{S \times d}$ spanning an invariant subspace of L^{-1}. By definition, there exists a block diagonal matrix $J_\Phi \in \mathbb{R}^{d \times d}$ such that $L^{-1}\Phi = \Phi J_\Phi$. Let $G \in O(S, T)$ spanning the top T invariant subspaces of L^{-1}. By definition, there exists a block diagonal matrix $J_G \in \mathbb{R}^{d \times d}$ such that $L^{-1}G = GJ_G$. Hencer, we have

$$
\begin{aligned}
(L^{-1}GG^\top)\Phi &= (L^{-1}G)G^\top\Phi \\
&= GJ_T G^\top\Phi \\
&= (\Phi J_\Phi) \text{ by orthonormality}
\end{aligned}
$$

Then, Φ is an invariant subspace of $L^{-1}GG^\top$. $\qquad\square$

F. Proofs for Subsection 4.2

We now proceed to the proof of Proposition 3. Before that, we introduce some necessary notations and lemmas.

F.1. Notations

Let $O(S, d) := \{A \in \mathbb{R}^{S \times d} : A^\top A = I\}$.

Definition 5. *Let $A, B \in O(S, d)$. The principle angles Θ between A and B are given by writing the SVD of $A^\top B = U \cos\Theta V^\top$.*

Definition 6. *Let $A, B \in O(S, d)$ with principle angles Θ. We define the distance $d(A, B)$ as $d(A, B) := \|\sin\Theta\|_{\mathrm{op}}$.*

Proposition 5. *Let $A, B \in O(S, d)$. We have the following identities:*

$$
d(A, B) = \|AA^\top - BB^\top\|_{\mathrm{op}} = \|\sin\Theta\|_{\mathrm{op}} = \|A^\top\bar{B}\|_{\mathrm{op}},
$$

where $\bar{B} \in O(S, S - d)$ satisfies $BB^\top + \bar{B}\bar{B}^\top = I$.

F.2. Approximate matrix decompositions

Lemma 9 (Deterministic error bound). *Let A be an $S \times S$ matrix. Fix $d \leqslant S$, and partition the SVD of A as:*

$$
A = \begin{bmatrix} U_1 & U_2 \end{bmatrix} \begin{bmatrix} \Sigma_1 & 0 \\ 0 & \Sigma_2 \end{bmatrix} \begin{bmatrix} V_1^\top \\ V_2^\top \end{bmatrix},
$$

where Σ_1 is $d \times d$ (the dimensions of all the other factors are determined by this selection). Put $A_d := U_1 \Sigma_1 V_1^\top$ as the rank-d approximation of A. Let Ω be an $S \times \ell$ test matrix ($\ell \geqslant d$). Put $Y = A\Omega$, $\Omega_1 = V_1^\top\Omega$ and $\Omega_2 = V_2^\top\Omega$. We have that:

$$
\|(I - P_Y)A_k\|_{\mathrm{op}}^2 \leqslant \|\Sigma_2\Omega_2\Omega_1^\dagger\|_{\mathrm{op}}^2.
$$

Proof. This proof is adapted from Theorem 9.1 of Halko et al. (2011).

Write $A_d = \hat{U}\hat{\Sigma}\hat{V}^\top$ the full SVD of A_d. By invariance of the spectral norm to unitary transformations,

$$
\|(I - P_Y)A_d\|_{\mathrm{op}}^2 = \|\hat{U}^\top(I - P_Y)\hat{U}(\hat{U}^\top A_d)\|_{\mathrm{op}}^2 = \|(I - P_{\hat{U}^\top Y})(\hat{U}^\top A_d)\|_{\mathrm{op}}^2
$$

Assume the diagonal entries of Σ_2 are not all strictly positive. Then Σ_2 is zero as a consequence of the ordering of the singular values.

$$
\mathrm{range}(\hat{U}^\top Y) = \mathrm{range}\begin{bmatrix} \Sigma_1\Omega_1 \\ 0 \end{bmatrix} = \mathrm{range}\begin{bmatrix} \Sigma_1 V_1^\top \\ 0 \end{bmatrix} = \mathrm{range}(\hat{U}^\top A_d)
$$

So we can conclude that $\|(I - P_Y)A_d\|_{\mathrm{op}}^2 = 0$ assuming that $V_1^\top$ and Ω_1 have full row rank.

Now assume that the diagonal entries of Σ_1 are strictly positive. Let $Z = \hat{U}^\top Y \cdot \Omega_1^\dagger \Sigma_1^{-1} = \begin{bmatrix} I_d \\ F \end{bmatrix}$ with $F = \Sigma_2 \Omega_2 \Omega_1^\dagger \Sigma_1^{-1} \in \mathbb{R}^{(S-d) \times d}$.

By construction, $\mathrm{range}(Z) \subset \mathrm{range}(\hat{U}^\top Y)$, hence we have,

$$\|(I - P_{\hat{U}^\top Y})(\hat{U}^\top A_d)\|_{\mathrm{op}}^2 \leqslant \|(I - P_Z)\hat{U}^\top A_d\|_{\mathrm{op}}^2 \leqslant \|A_d^\top \hat{U}(I - P_Z)\hat{U}^\top A_d\|_{\mathrm{op}} \leqslant \|\hat{\Sigma}(I - P_Z)\hat{\Sigma}\|_{\mathrm{op}}$$

Following the proof from Theorem 9.1 of Halko et al. (2011), we have

$$(I - P_Z) \preccurlyeq \begin{bmatrix} F^\top F & B \\ B^\top & I_{S-d} \end{bmatrix}$$

where $B = -(I_d - F^\top F)^{-1} F^\top \in \mathbb{R}^{d \times (S-d)}$.

Consequently, we have

$$\hat{\Sigma}(I - P_Z)\hat{\Sigma} \preccurlyeq \begin{bmatrix} \Sigma_1 F^\top F \Sigma_1 & 0 \\ 0 & 0 \end{bmatrix}$$

$\hat{\Sigma}(I - P_Z)\hat{\Sigma}$ is PSD by the conjugation rule, hence the matrix on the right hand side is PSD too. It follows that

$$\|\hat{\Sigma}(I - P_Z)\hat{\Sigma}\|_{\mathrm{op}} \leqslant \|\Sigma_1 F^\top F \Sigma_1\|_{\mathrm{op}} = \|F\Sigma_1\|_{\mathrm{op}}^2 = \|\Sigma_2 \Omega_2 \Omega_1^\dagger\|_{\mathrm{op}}^2$$

$\square$

Lemma 10 (Average spectral error). *Let A be an $S \times S$ matrix with singular values $\sigma_1 \geqslant \sigma_2 \geqslant \dots$. Fix a target rank $2 \leqslant d \leqslant S$ and an oversampling parameter $p \geqslant 2$ where $p + d \geqslant S$. Draw and $S \times (d+p)$ standard gaussian matrix Ω and construct the sample matrix $Y = A\Omega$. Then, we have*

$$\mathbb{E}\|(I - P_Y)A_d\|_{\mathrm{op}} \leqslant \sqrt{\frac{d}{p-1}}\sigma_{d+1} + \frac{e\sqrt{d+p}}{p}\left(\sum_{j=d+1}^{S} \sigma_j^2\right)^{1/2}.$$

Proof. By Lemma 9 and linearity of the expectation, we have

$$\mathbb{E}\|(I - P_Y)A_d\|_{\mathrm{op}} \leqslant \mathbb{E}\|\Sigma_2 \Omega_2 \Omega_1^\dagger\|_{\mathrm{op}}$$

$$\leqslant \sqrt{\frac{d}{p-1}}\sigma_{d+1} + \frac{e\sqrt{d+p}}{p}\left(\sum_{j=d+1}^{S} \sigma_j^2\right)^{1/2},$$

where the last inequality comes from Theorem 10.6 of Halko et al. (2011). $\square$

Lemma 11. *Let $A \in \mathbb{R}^{m \times n}$, and fix a $d < n$. Let $\sigma_1 \geqslant \sigma_2 \geqslant \dots \geqslant \sigma_n$ denote the singular values of M listed in decreasing order, and suppose that $\sigma_k > 0$. Let A_d denote the rank-d approximation of A. Fix any matrix $Y \in \mathbb{R}^{m \times T}$. We have:*

$$\|(I - P_Y)A_k\|_{\mathrm{op}} \geqslant \|(I - P_Y)P_{A_k}\|_{\mathrm{op}}\sigma_k.$$

Proof. Decompose $P_Y^\perp A_k$ as:

$$P_Y^\perp A_k = P_Y^\perp P_{A_k} A_k$$

$$\|P_Y^\perp A_k\|_{\mathrm{op}} = \|P_Y^\perp P_{A_k} A_k\|_{\mathrm{op}} \geqslant \|P_Y^\perp P_{A_k}\|_{\mathrm{op}}\|A_k\|_{\mathrm{op}} = \|P_Y^\perp P_{A_k}\|_{\mathrm{op}}\sigma_k$$

where the inequality comes from the sub-multiplicativity of the the operator norm $\square$

Proposition 6. *Let A be an $S \times S$ matrix with singular values $\sigma_1 \geqslant \sigma_2 \geqslant ....$ Fix a target rank $2 \leqslant d \leqslant n$ and an oversampling parameter $p \geqslant 2$ where $p + d \geqslant S$. Draw and $n \times (d + p)$ standard gaussian matrix Ω and construct the sample matrix $Y = A\Omega$. Then, we have*

$$\mathbb{E}\|(I - P_Y)P_{A_d}\|_{\mathrm{op}} \leqslant \sqrt{\frac{d}{p-1}} \frac{\sigma_{d+1}}{\sigma_d} + \frac{e\sqrt{d+p}}{p} \left(\sum_{j=d+1}^{S} \frac{\sigma_j^2}{\sigma_d^2} \right)^{1/2}.$$

Proof. By Lemma 11 and linearity of the expectation, we have

$$\frac{1}{\sigma_d} \mathbb{E}\|(I - P_Y)A_d\|_{\mathrm{op}} \geqslant \mathbb{E}\|(I - P_Y)P_{A_d}\|_{\mathrm{op}}$$

Now applying Lemma 10, we have

$$\sqrt{\frac{d}{p-1}} \frac{\sigma_{d+1}}{\sigma_d} + \frac{e\sqrt{d+p}}{p} \left(\sum_{j=d+1}^{S} \frac{\sigma_j^2}{\sigma_d^2} \right)^{1/2} \geqslant \mathbb{E}\|(I - P_Y)P_{A_d}\|_{\mathrm{op}}$$

$\square$

Observe that, as the oversampling factor p grows, the RHS tends to zero. However, the dependence will be something like $p \gtrsim 1/\varepsilon^2$, if you want the RHS to be $\leqslant \varepsilon$. This actually makes sense I think– you are using concentration of measure to increase the accuracy, so you should pay $1/\varepsilon^2$ sample complexity.

F.3. Analysis

Proposition 3 (MC Error bound). *Let $G \in \mathbb{R}^{S \times T}$ be a sample from a standard gaussian distribution and assume $d \leqslant T$. Let F_d be the top-d left singular vectors of the successor representation $(I - \gamma P^\pi)^{-1}$ and $\hat{F}_d$ be the top left singular vectors of $(I - \gamma P^\pi)^{-1}G$. Denote $\sigma_1 \geqslant \sigma_2 \geqslant ... \geqslant \sigma_S$ the singular values of the SR and $\mathrm{dist}(F_d, \hat{F}_d)$ the $\sin\theta$ distance between the subspaces spanned by F_d and $\hat{F}_d$. Denoting $p = T - d$, we have*

$$\mathbb{E}[\mathrm{dist}(F_d, \hat{F}_d)] \leqslant \sqrt{\frac{d}{p-1}} \frac{\sigma_{d+1}}{\sigma_d} + \frac{e\sqrt{T}}{p} \left(\sum_{j=d+1}^{n} \frac{\sigma_j^2}{\sigma_d^2} \right)^{\frac{1}{2}}$$

Proof. Let $l \in \{d,...,S\}$. $F_l \in O(S, l)$ be the top l left singular vectors of $(I - \gamma P^\pi)^{-1}$ and $\hat{F}_l \in O(S, d)$ be the top left singular vectors of $(I - \gamma P^\pi)^{-1}G$.

$$
\begin{aligned}
d(F_d, \hat{F}_d) &= \|\hat{F}_d^\top F_d^\perp\|_{\mathrm{op}} \\
&= \|P_{\hat{F}_d} P_{F_d}^\perp\|_{\mathrm{op}} \\
&\leqslant \|P_{L^{-1}G} P_{F_d}^\perp\|_{\mathrm{op}} \text{ as } \mathrm{span}(\hat{F}_d) \subseteq \mathrm{span}(L^{-1}G) \\
&= \|\hat{F}_T^\top F_d^\perp\|_{\mathrm{op}} \\
&= \|F_d^\top \hat{F}_T^\perp\|_{\mathrm{op}} \\
&= \|P_{F_d} P_{\hat{F}_T}^\perp\|_{\mathrm{op}} \\
&= \|P_{\hat{F}_T}^\perp P_{F_d}\|_{\mathrm{op}} \text{ by symmetry of the projection matrices} \\
&= \|(I - P_{\hat{F}_T}) P_{F_d}\|_{\mathrm{op}} \\
&= \|(I - P_{L^{-1}G}) P_{(L^{-1})_d}\|_{\mathrm{op}} \\
&\leqslant \frac{1}{\sigma_d} \|(I - P_{L^{-1}G})(L^{-1})_d\|_{\mathrm{op}} \text{ by Lemma 11}
\end{aligned}
$$

Now taking the expectation with respect to G and applying Proposition 6,

$$\mathbb{E}[d(F_d, \hat{F}_d)] \leqslant \sqrt{\frac{d}{T-d-1}} \frac{\sigma_{d+1}}{\sigma_d} + \frac{e\sqrt{T}}{T-d} \left(\sum_{j=d+1}^{n} \frac{\sigma_j^2}{\sigma_d^2} \right)^{1/2}.$$

$\square$

G. n-step TD case

We now provide intuition about how our theory extends from 1-step to n-step temporal difference learning. The n-step TD loss corresponds to the following loss

$$\mathcal{L}_{\text{aux}}^{\text{TD}}(\Phi, W) = \left\| (\Xi)^{\frac{1}{2}} \left(\Phi W - \text{SG} \left(\sum_{k=0}^{n-1} \gamma^k (P^\pi)^k G + \gamma^n (P^\pi)^n \Phi W \right) \right) \right\|_F^2$$

Our analysis mostly stays the same, with the exception that the successor representation $(I - \gamma P^\pi)$ becomes $(I - \gamma^n (P^\pi)^n)$ and the cumulant matrix G becomes $G_n = \sum_0^{n-1} \gamma^k (P^\pi)^k G$. Following the same proof strategy as that of Lemma 1, we find that the critical representation are given by the real invariant subspaces of $(I - \gamma^n (P^\pi)^n)^{-1} G_n G_n^\top \Xi$. Now following the proof strategy from Theorem 1 shows that all non-top real invariant subspaces of $(I - \gamma^n (P^\pi)^n)^{-1} G_n G_n^\top \Xi$ are unstable. This implies that the n-step TD algorithm also converges towards a real top-d invariant subspace of or diverges with probability 1.